Applied Energy 202 (2017) 507–526

Contents lists available at ScienceDirect

Applied Energy

journal homepage: www.elsevier.com/locate/apenergy

Design and experimental development of a compact and efficient range extender engine

Massimo Borghi, Enrico Mattarelli, Jarin Muscoloni, Carlo Alberto Rinaldini *, Tommaso Savioli, Barbara Zardin

Engineering Department "Enzo Ferrari", University of Modena and Reggio Emilia, Via Vivarelli 10, 41125 Modena, Italy

HIGHLIGHTS

- New concept of compact, clean and fuel efficient range extender engine.
- Developments through CFD simulation and experiments.
- Significant step forward in comparison to the current 4-strokes.
- Weight: −35%, brake efficiency: +6%, heat rejected: −18%, thermal load: −40%.
- Cost effective technology for CO_2 reduction in transportation.

ARTICLE INFO

Article history:
Received 22 March 2017
Received in revised form 15 May 2017
Accepted 18 May 2017

Keywords:
CFD simulation
2-Stroke
Range extender
GDI
Electric supercharger

ABSTRACT

The paper reviews the design and experimental development of an original range-extender single-cylinder two-stroke gasoline engine, rated at 30 kW (maximum engine speed: 4500 rpm). The goal of the project is to get most of the benefits of the two-stroke cycle (compactness, high power density, low cost), while addressing the typical issues affecting the conventional engines of this type. Among many recent similar propositions, the peculiarities of this engine, besides the cycle, are: external scavenging by means of an electric supercharger, piston controlled scavenge and exhaust ports (no poppet valves), gasoline direct injection (GDI), and a patented rotary valve for the optimization of the scavenging process, of the loop type. Lubrication is identical to a conventional four-stroke engine, and the rotary valve, connected to the crankshaft, helps to improve the balance of the piston reciprocating forces, yielding an excellent NVH behavior. It should be noted that, except the patented rotary valve, all the engine parts are standard automotive commercial components, that don't require any specific expensive technology. In fact, the originality of the engine consists in the optimum combination of existing well assessed concepts.

The scavenging and combustion systems of the engine are developed in the first phase of the project, including the construction and the experimental testing of a prototype. In the second phase, the air metering system of the prototype is completely modified: the piston pump is replaced by an electric supercharger, and engine load is now controlled by the supercharger speed, without throttle valve.

The new engine is compared to a standard 4-stroke engine, developed in a previous project for the same application. The main advantages of the two-stroke engine may be summarized as follows: lower weight (−35%), higher brake efficiency (+6%, on average), less heat rejected (−18%), lower thermal and mechanical loads within the cylinder (−40%). The only concern, that will be addressed in a future phase of the study, is the compliance with very low NOx limits: in the worst scenario, the 2-stroke engine could be forced to adopt a well assessed but expensive after-treatment device.

1. State of the art

One of the most critical challenges of recent electric cars is the driving range achievable with the current battery technology, which allows the vehicle to store only a small fraction of the

* Corresponding author.
E-mail address: carloalberto.rinaldini@unimore.it (C.A. Rinaldini).

http://dx.doi.org/10.1016/j.apenergy.2017.05.126
0306-2619/

Nomenclature

Acronyms

BDC	bottom dead center
BMEP	brake mean effective pressure
BSFC	brake specific fuel consumption
CCD	charge control device
CFD	computational fluid dynamics
EGR	exhaust gas recirculation
GDI	gasoline direct injection
HCCI	homogeneous charge compression ignition
IMEP	indicated mean effective pressure
MBT	maximum brake torque
NVH	noise, vibration, harshness
OEM	original equipment manufacturer
SPL	sound pressure level
TDC	top dead center

energy provided by conventional fuels, such as gasoline or diesel. An effective way to address the so called "range anxiety" is the adoption of a range extender, that is a small internal combustion engine designed to recharge the traction batteries when their available energy content drops below a specified threshold [1]. The range extender is also a practical solution to further issues. As an example, the range extender enables a more efficient use of heating and air-conditioning functions when the vehicle stops, thus helping to further reduce CO_2 emission [2].

The basic requirements for the range extender are:

- peak power sufficient to allow the car to reach a target highway speed (typically, 120 km/h), with empty batteries;
- compactness and lightness, in order to permit an easy and not expensive installation on a conventional vehicle;
- excellent fuel efficiency, to maximize the benefits on CO_2 reduction of the electric vehicle;
- low pollutant emission levels, to meet stringent regulations;
- excellent NVH behavior: ideally, the driver should not be able to tell when the combustion engine is running;
- low cost.

For vehicles needing a power higher than 40–50 kW, a range extender can be directly derived from a mass production engine. Conversely, for city cars requiring less than 30 kW, even the smallest existing automotive engine is not suitable. Apparently, the easiest solution is to convert engines, already existing for other applications (motorcycles, small gen-sets, etc.), into range extenders. However, the engineering cost for these conversions would be not much lower than a development from scratch. Moreover, a specifically developed engine allows the designer to select more suitable technologies and solutions. This is the reason why some important players of the automotive industry, not only OEMs, decided to develop their own Range Extender.

As a first example, Lotus Engineering [3] developed a 3 cylinder, naturally aspirated, 1.2 l, 4 stroke engine, able to deliver a maximum power of 35 kW at 3500 rpm. The engine weight, without generator and related electric/electronic parts, is about 56 kg.

In the GETRAG range extender [4], the number of cylinders and the engine displacement are reduced to 2 and 0.9 l, respectively, while the target of 45 kW at 3500 rpm is achieved by means of a turbocharger. In this solution the engine is connected by a 2 speed gearbox to the differential and it is also able to provide mechanical power for the vehicle traction and not only for the generation of electric current. The engine weight is almost identical to the Lotus solution (55 kg).

The two-cylinder 4-Stroke layout was selected also by Mahle for their prototype [5]: the engine is naturally aspirated, and it reaches 40 kW of maximum power at 4000 rpm. Besides a very low weight of the engine, 50 kg, Mahle also claims an excellent best specific fuel consumption of 240 g/kWh.

Another compact two-cylinder, naturally aspirated unit is proposed by FEV and KSPG [6]. The power target of 30 kW at 4500 rpm is achieved with a lower displacement (800cc). Differently from Mahle, FEV decided to adopt an in-line layout, and to use the coupled electric motor to balance the inertia forces.

In parallel to conventional solutions, AVL and FEV are developing some prototypes based on the rotary engine technology [7,8]. While AVL developed a 250cc engine, able to deliver 15 kW at 5000 rpm, FEV opted for a larger capacity (295cc), achieving 18 kW at 5500 rpm. These solutions are much more compact of an equivalent 4 stroke, and they have the indisputable benefit of very low vibrations. However, the proposed prototypes don't seem to introduce any particular innovation to the conventional rotary engine technology, which is still penalized in terms of pollutant emissions and high specific fuel consumption. Moreover, reliability and performance of this technology are directly related to the expensive manufacturing process of some key parts; this issue makes the production costs increase, being the predictable market volumes of such systems quite low, compared to standard automotive figures.

Micro gas turbines are interesting propositions too [9], but they appear to be still immature for an immediate application, being their main challenges not entirely solved.

4-Stroke Diesel engines are normally discarded as range extenders, because of their low power-weight ratio, poor NVH characteristics, as well as for the high cost of their exhaust after-treatment systems.

2. Two-stroke engines?

The two-stroke cycle, with a new specific design, represents an unconventional but not exotic alternative to 4-Strokes. The main reason of interest for this type of machines is the double cycle frequency, allowing the designer to either draw a very compact and light unit for the given power target, or limit the maximum rotational speed, with ensuing advantages in terms of mechanical efficiency, noise and vibrations.

Recently, the modernization of the two-stroke engine is a quite hot research topic worldwide, so that it would be impossible in this paper to review all the relevant propositions. Only the most similar to the current project will be presented here, whereas for a more complete overview, one can refer to [10].

A 2-Stroke engine can easily share many technologies and components with a Spark Ignition (SI) passenger car engine. Abandoning the crankcase pump, the lubrication system (oil sump, pump, internal passages) can be the same. Moreover, a commercial high pressure gasoline direct injection system (GDI) can be installed also on a 2-Stroke. Finally, a 2-Stroke prototype can be constructed on the basis of an existing 4-Stroke, modifying only the valves actuation strategy, as done by some researchers [11–12].

The adoption of a modern GDI system is a strong help, but its implementation in a 2-stroke engine is far from trivial. In particular, the position of the injector nozzle and its geometry must be carefully selected. The main issue, in comparison to a 4-Stroke, is the limited time available for achieving a proper air-fuel mixture within the cylinder, before combustion onset: in order to avoid the loss of fuel at the exhaust, injection can't start before bottom dead center, as generally done in conventional automotive engines, then air-fuel mixing must be much faster. However, in a 2-stroke valve-less loop scavenged engine, the combustion system design, including the injector position, is almost free of constraints; furthermore, properly designed piston controlled ports are able to generate a strong turbulence within the cylinder, enhancing the mixing process: finally, a range extender does not typically operate over 4500 rpm, for NVH reasons.

As reported by many authors [12–20], direct injection, even at relatively low pressure, strongly helps a 2-stroke SI engine to address most of the typical issues related to fuel consumption and emissions. Hydrocarbon emissions can be dramatically reduced, and the adoption of a conventional three-way catalyst enables the abatement of CO and HC to the levels of equivalent 4-strokes. Engine-out NOx remains very low, due to the charge dilution with residuals.

When stringent emission regulations are enforced, at high loads and speeds, a standard 3-way catalyst coupled with an accurate fuel metering system may not be enough. In particular, the NOx concentration after the catalyst may be higher than desired, due to the peaks of oxygen concentration in the exhaust flow occurring at the end of the scavenging process (short-circuit cannot be avoided in a 2-Stroke engine, and the instantaneous air excess is expected to freeze the reduction of NOx in the catalyst). The lower is the trapping efficiency, the stronger is this negative effect. Fortunately, for the most part of the exhaust process the Oxygen concentration in the catalyst is the same of a 4-Stroke engine since short circuit generally occurs only at the end of scavenging.

Very encouraging emissions results have been found by the researchers at LOTUS [21–22], in the "Omnivore" project, a two stroke, loop scavenged, direct injected, variable compression ratio engine, able to operate with different fuels even in HCCI modes.

It should be noted that the presence of air in the exhaust flow can be turned into an advantage during the engine warm-up phase: setting a slightly rich mixture within the cylinder, the additional fuel may burn in the catalyst, strongly reducing the light-off time. Therefore, the catalyst may be placed relatively far from the cylinder, leaving more freedom for fluid-dynamic tuning and packaging.

The constraints on overall dimensions and cost make the use of poppet valves not attractive for a two-stroke range extender. Conversely, piston controlled ports enable a very compact and light cylinder design, while reducing the flow losses across the cylinder. Among several options, loop scavenging seems preferable to an opposed piston design, such as the one discussed in [23], since it requires a single crankshaft (instead of two), and it leaves complete freedom for the design of the combustion chamber.

Summarizing the above mentioned considerations, the keys for a cost effective 2-stroke range extender are:

- piston controlled ports, loop scavenging;
- capability to control and optimize the scavenging process;
- high rates of internal EGR, even at high load, in order to reduce in-cylinder Nitrogen oxides concentration;
- optimum air-fuel mixing, that can be achieved by means of high turbulence levels and proper injection strategies;
- no lubrication oil within the cylinder.

Finally, it is important to bear in mind that a Range Extender engine is operated only at a few steady points. Therefore, the optimization is much easier, and potentially critical operations for emissions, reliability or fuel consumption may be simply discarded from the set of working points.

3. The proposed engine

The engine analyzed in this study is a 2-Stroke GDI supercharged unit, rated at 30 kW (64 Nm) at 4500 rpm, developed by PRIMAVIS. The goal of the paper is to assess its potential as a range-extender. It should be noted that the maximum engine speed is limited by NVH issues, and the power target is ideal for a C-segment passenger car.

3.1. Layout

The first step of the project, started in 2012, was the choice of the scavenging type. Crankcase scavenging was immediately discarded, because of the lubrication oil dispersed in the fresh charge and bypassing the cylinder, as well as for the increase of friction losses and wear at high load. Conversely, an external compressor enables the use of a conventional and efficient oil sump, leaving a lot of freedom in the choice of the induction and exhaust systems.

Most of externally scavenged engines have Roots-type blowers, but other solutions are possible. As in the Ricardo Dolphin engine [23], or in the more recent ALCOR [24], an additional cylinder can be adopted for pumping air from ambient to the power cylinder; the second piston also enables an excellent balance of the crankshaft, as occurs in a V2-90° 4-Stroke engine. The drawbacks of this solution are the increase of overall dimensions and the need of automatic valves installed in the pump head.

An alternative solution for external scavenging is represented by electric superchargers, recently adopted as a support to conventional turbocharging [26–30]. When the required power is low, these machines can be very compact; furthermore, they don't need an additional battery pack, being a big one already installed on the electric vehicle.

In 2014, PRIMAVIS built and tested a first prototype adopting a piston pump with different types of automatic valves installed in the pump head. The project is described in detail in some technical reports [31–34], and the prototype is visible in Fig. 1.

The experimental campaign revealed that automatic valves are quite critical, in terms of reliability and performance: therefore, in 2016 it was decided to move from a piston pump to an electric supercharger.

3.2. The patented valve

The capability of a 2-Stroke engine to operate with piston controlled ports is a significant advantage in terms of compactness and cost, but it also yields some downsides. As well known, it is difficult to limit the short-circuit of fresh charge across the cylinder, especially at low engine speeds; another problem may be the presence of large residual gas "pockets" within the cylinder, after exhaust port closing. Finally, a number of minor issues must be addressed when designing the piston-rings-liner assembly (high wear of rings, poor liner lubrication, etc.).

A fundamental help to improve the scavenging process in a cylinder with piston controlled ports can be obtained from a rotary valve called "Charge Control Device" (CCD) patented by PRIMAVIS [35]. The valve, visible in Fig. 2, is made up of a rotor, mounted on roller bearings and revving at the same speed of the engine. It controls the flow through a set of auxiliary transfer ports opposite to

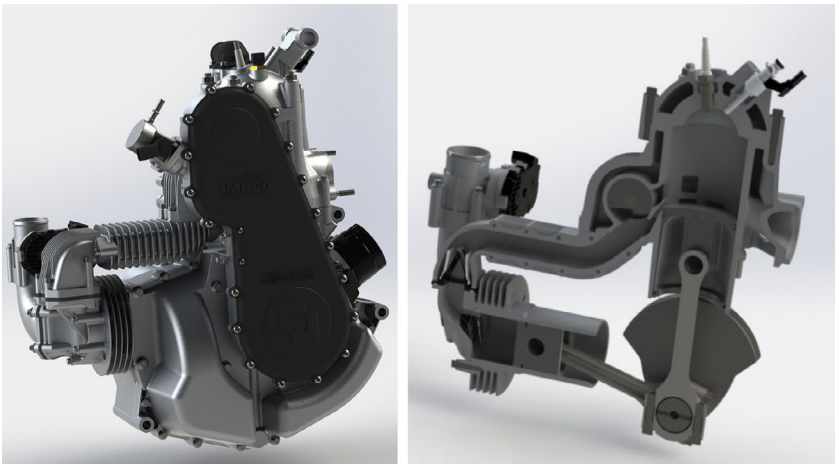

Fig. 1. Views of the first prototype built by PRIMAVIS [31–34].

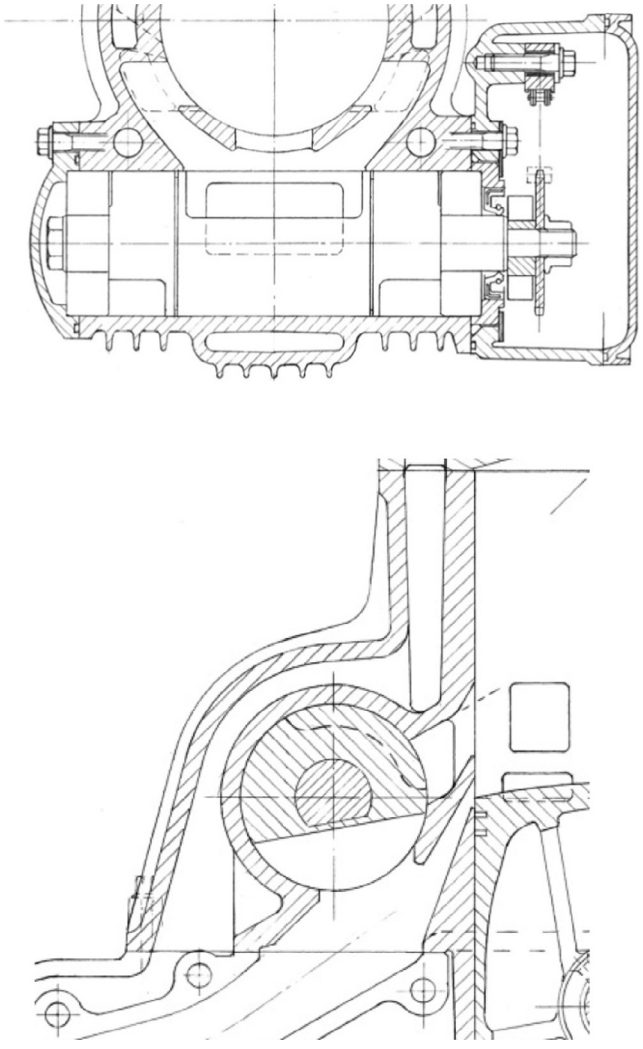

Fig. 2. Installation of the CCD valve [33].

the exhaust ports, and it allows the designer to define the time-area diagram in a quite free manner. In particular, it is possible to adopt asymmetric timings, able to increase the amount of fresh charge stuffed within the cylinder, while contemporarily reducing the short-circuit. It is important to notice that the installation of CCD does not generate critical constraints on ports design, that can rely on the well-established engineering practice on 2-S high speed engines.

4. Basic engine design

The optimization of the scavenging and combustion system is the most critical part of the project, and it requires a strong support from both CFD simulation and experiments. CFD-simulation plays a key role to address the design process, while keeping the development cost under control. The followed approach is presented in Fig. 3.

A first cylinder design is defined on the basis of the standard engineering practice, and refined by means of an iterative process, including both 1D and 3D CFD simulations. For 1D engine thermo-fluid-dynamic numerical analyses, a well assessed commercial software is used (GT-Power), while for 3D calculations a customized version of the KIVA-3V code is employed. Two types of multi-dimensional investigations are required, the former focused only on the scavenging process, the latter encompassing the whole engine cycle, including spray and combustion.

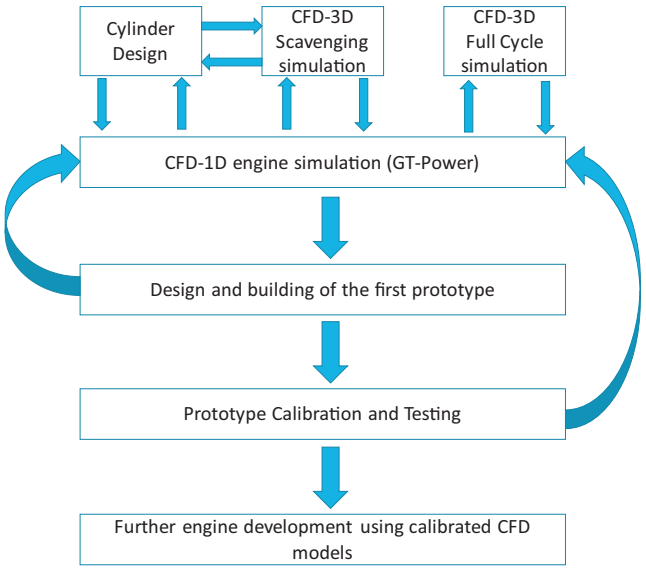

Fig. 3. Design methodology.

4.1. CFD-3D scavenging simulation

The scavenging simulation provides some fundamental information required by the GT-Power model, such as the discharge properties of the ports, as well as the correlation between the composition of the charge within the cylinder and the composition of the gas leaving the cylinder through the exhaust ports. Moreover, a 3D scavenging analysis allows the designer to get a very detailed insight of the cylinder flow patterns, enabling a further optimization of ports design. The CFD-3d scavenging analysis starts from the opening of the first port (generally the exhaust one) and terminates after the closure of the last port (in this case, the auxiliary ports controlled by the CCD valve). Fuel injection and combustion are not included in this analysis, therefore initial conditions (pressure, temperature, composition of the charge) must be provided by a parallel GT-Power simulation, and they should be corrected by means of some iterations, until the mass within the cylinder at the beginning of the calculation corresponds to the final mass after the scavenging process (adding the fuel mass, injected after ports closing). Three simulation cycles are generally sufficient to get a satisfactory agreement (mass difference less than 2%).

A view of the computational mesh used in these simulations is shown in Fig. 4. At bottom dead center (BDC) the grid is made up of about 100,000 cells, whose typical dimension in the ports region is about 1 mm. The grid set-up is based on the experience gained on many similar projects [36–43], where the numerical models are calibrated with the support of experimental data.

The scavenging system quality may be assessed by plotting the calculated values of trapping efficiency as a function of delivery ratio. The intensity of the tumble vortex within the cylinder is also fundamental to assess the engine potential to achieve a good air-fuel mixing. The above mentioned parameters are defined as follows:

Delivery ratio: instantaneous ratio of the mass delivered through the scavenge ports to a reference mass.

Trapping efficiency: instantaneous ratio of the fresh charge mass trapped within the cylinder to the mass delivered through the scavenge ports.

Reference mass: defined as the product of fresh charge density and engine unit displacement.

Tumble ratio: Ratio of the average angular speed of the tumble vortex to the engine angular speed. The vortex angular speed is calculated as the ratio of the angular momentum referred to the axis orthogonal to the symmetry plane and passing through the center of mass, to the moment of inertia, referred to the same axis.

A characterization of the scavenging process, based on CFD-3D simulation, is presented in Figs. 5 and 6. For a complete description of this study, one can refers to [39].

Fig. 5 compares the trapping efficiency curves calculated at three different engine speeds (2500, 4000 and 5500 rpm) to two ideal curves: perfect displacement and perfect mixing. A perfect displacement is the most desirable condition, and it can be obtained when the fresh charge sweeps the cylinder without mixing with the exhaust gas and without short-circuit. A less good situation occurs when the fresh charge mixes with the exhaust gas, generating a uniform distribution within the cylinder (perfect mixing). An efficient scavenge system should coincide as long as possible with a perfect displacement, and perform always better than a perfect mixing. The curves of Fig. 5 shows a quite satisfactory behavior of the proposed scavenging system.

Another important confirmation about the effectiveness of the scavenge system is given by plotting the in-cylinder turbulence, Fig. 6. The tumble ratios within the cylinder are about two times higher than those typically found in 4-stroke GDI engines. As a result, the air-fuel mixing process is expected to be strongly enhanced.

4.2. CFD-3D full cycle simulation

Once the ports geometry is "frozen", full cycle CFD-3D analyses are employed to investigate the spray and combustion processes. Again, the support of GT-Power is fundamental, in order to provide accurate boundary conditions when the ports are open.

The most critical operating condition is at maximum engine speed (4500 rpm), full load: here, the time available for fuel evaporation and mixing is minimum, and the amount of fuel is the maximum one. In order to guarantee a regular combustion, it is necessary to achieve a homogeneous air-fuel mixture at about 20° before Top Dead Center. Failing this goal means not only a poor combustion efficiency, but also a high risk of knocking (where mixture is lean, temperature is generally higher, and auto-ignition may occur more easily). The composition of the charge before TDC depends on a huge number of variables: engine speed, delivery

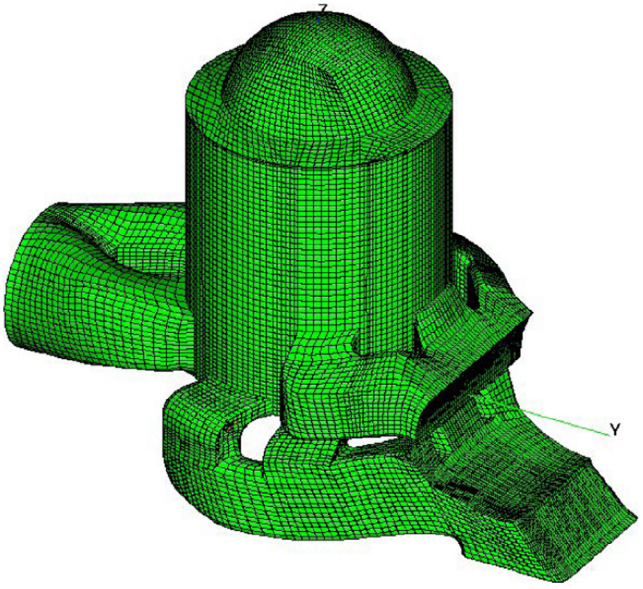

Fig. 4. View of the computational grid at BDC, employed for scavenging simulations.

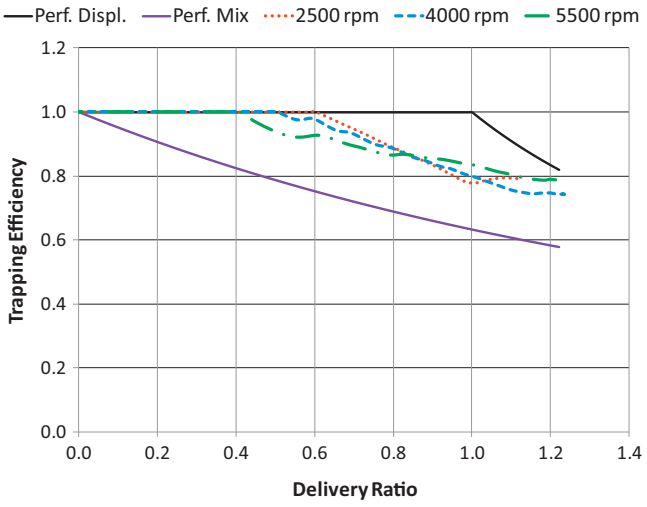

Fig. 5. Trapping efficiency as a function of delivery ratio, calculated at different engine speeds. Perfect displacement and perfect mixing curves are also shown.

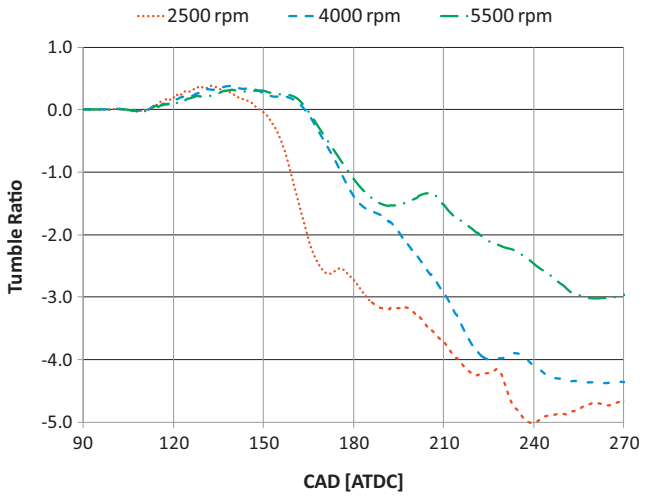

Fig. 6. Tumble ratio calculated at different engine speeds.

ratio, injector nozzle geometry and position, injection strategy (pressure and timing), air-fuel ratio... In order to limit these variables, only one commercial injector has been considered (Magneti Marelli RDI 206); moreover, the maximum injection pressure is set at 200 bar, as in standard automotive applications.

The experimental characterization in a closed vessel of the selected injector is compared to a correspondent KIVA simulation in Figs. 7 and 8. As visible, the numerical spray model yields reliable outputs, from both a qualitative and a quantitative point of view. In particular, the average droplet dimension (20 μm) is consistent with the data provided by the injector manufacturer.

Figs. 9–12 present a selection of results from a CFD-3D simulation of the whole engine cycle at 4500 rpm, full load. Fuel concentration and gas temperature are plotted on the symmetry plane, at different crank angles (from BDC, to 10° after TDC). The injection pressure is set at 200 bar, and the fuel is introduced into the chamber by means of a single shot, beginning at 10° before BDC (or 170 cad after TDC), and stopping at about 20 cad after BDC. The average trapped air-fuel ratio is stoichiometric, and about 15% of the trapped mass is made up of residual gas.

From the analysis of Fig. 9, the following considerations can be made:

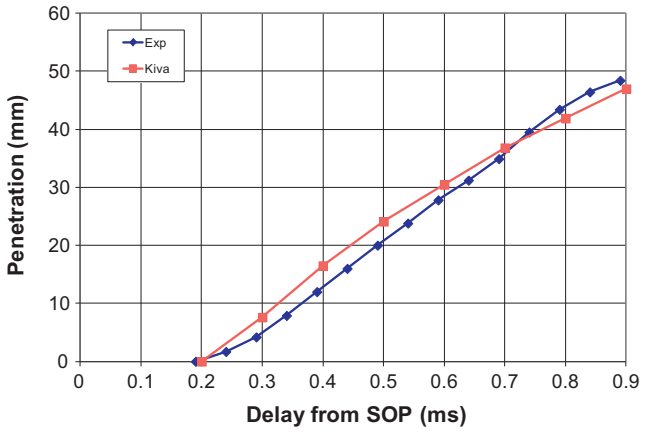

Fig. 7. Comparison between experimental and numerical results in terms of spray penetration (Injector MM RDI 206).

- despite the fact that the exhaust port is open during the whole injection process, no fuel is lost, thanks to the strong turbulence, able to confine the air-fuel mixture in the upper region of the cylinder, far from the outlet port;
- the above described behavior is one of the main targets of the ports optimization: in fact, advancing the injection start without losing fuel is the key to achieve a good air-fuel mixing at high engine speed
- the cylinder local temperature depends on both the presence of fresh charge and the vaporization of the fuel: it's highly desirable to achieve a homogeneous air-fuel mixture before top dead center in order to avoid pockets of hot gas, with ensuing problems of auto-ignition.
- no fuel impingement is observed: this is very important, in order to avoid the formation of particulate, and the ensuing necessity of an expensive gasoline particulate filter;
- the amount of fresh charge lost through the exhaust up to 210 cad after TDC is negligible

Fig. 10, shows how the fuel vapor formed in the head region is diffusing within the cylinder. The dimension of the ultra-rich region close to the injector quickly decreases, and the red cloud is dragged downward by the cylinder turbulence. It is interesting to notice that, at 290 cad after TDC, there is still a stratification of the air-fuel mixture, rich on the left, lean on the right. However, this situation is set to change, as the piston approaches top dead center. Another important information provided by Fig. 10 is the presence of a pocket of residual gas trapped within the cylinder at exhaust port closing (70 cad after BDC). This pocket is the result of the exhaust back-flow occurring between the closure of the conventional transfer ports (about 35° after BDC) and the closure of the exhaust port; the backflow is due to the so-called "plugging wave", generated by the reflection of compression waves in the exhaust system, highly desirable to achieve a good trapping efficiency. The strong cylinder turbulence immediately dilutes the exhaust gas pocket within the fresh charge: the best evidence of the quick mixing is the almost uniform temperature distribution at 290 cad after TDC (110° after BDC).

Fig. 11 is focused on the mixing process during the compression stroke, before combustion. At 20 cad before TDC the charge is ready to burn: the temperature is uniform (about 800 K), and the fuel distribution quite homogeneous. It may be observed that the right part of the chamber is slightly richer than the left: this difference is set to have a strong relevance for the following combustion, since the flame will be faster in the richer region.

Finally, Fig. 12 shows a large portion of the combustion process. Spark ignition occurs at 10 cad before TDC, but its effects are visible only 5 cad before TDC. The flame front is propagating very fast, especially at the right side, and the chamber is almost completely swept just 10° after TDC. The high burn rate predicted by the CFD simulation is fully confirmed by the experimental tests, presented in the next section.

As far as combustion is concerned, it is important to notice that in the most critical operating condition (maximum speed and load, high dilution of the charge with residuals) the engine does not present any problem, on the contrary, combustion seems very fast and efficient.

At the moment of writing this paper no attempt has been made to control the pollutant emissions, being impossible at this stage of the project to define a set of reference operating conditions without a deep analysis of the engine-vehicle matching. As well known, the engine working conditions mainly depend on the total mass of the electric car, on the reference driving cycle, on the specific customer requirements, and on the choice of the after treatment system. From a qualitative point of view, the 3D-CFD simulations reveal that NOx emissions are much lower than a correspondent

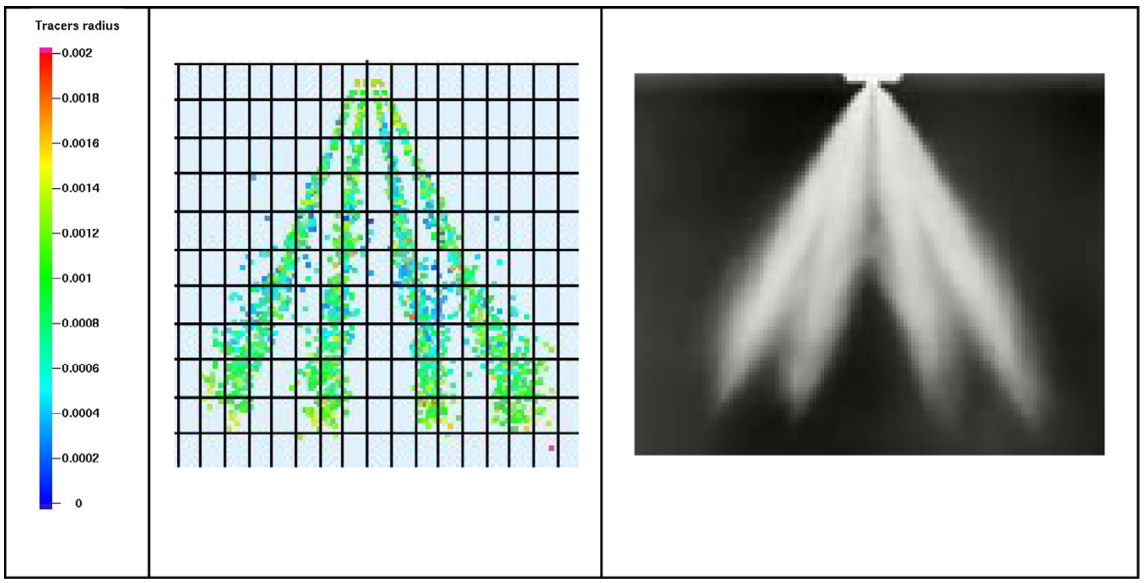

Fig. 8. Qualitative comparison between experiments and simulation, considering a time of 0.4 ms after start of pulse. The scale colors correspond to droplet dimensions (cm).

4-stroke engine, while the other pollutants are comparable. No soot is observed.

5. Calibration of engine models

An experimental campaign has been recently carried out at the Department of Engineering "Enzo Ferrari" (University of Modena and Reggio Emilia), on the 2-Stroke prototype described in the previous sections and built by PRIMAVIS. The experimental facility has been comprehensively described in previous papers [44,45], so that only the fundamentals will be reviewed here. The testing bed features an Apicom FR 400 BRV eddy-current brake and the Apicom Horus software for system control and data acquisition. Besides the standard pressure and temperature transducers, the laboratory instruments also include flow meters for measuring air and fuel consumption, and a Lambda sensor. A high frequency indicating system has been specifically designed and installed in order to record in-cylinder pressure traces; the system is made up of a Kistler piezoelectric transducer, integrated in the spark plug, a charge amplifier and an optical encoder. Pressure and phase signals are processed by means of the NI CompactRIO hardware and the Alma Automotive software (Obi). The experimental uncertainty of the measures is reviewed in Table 1

In the engine installation, particular care is devoted to the design of the junction between engine and brake: on the one hand, a stiff junction is desirable to avoid resonance effects, that can cause mechanical failures, even when occurring for a short time; on the other hand, engine vibrations must be properly dumped, by including elastic elements in the junction.

The main goal of the experimental campaign is to validate the CFD numerical models employed in the design of the prototype. In particular, the collected data enable the accurate calibration of the GT-Power engine model, already including the results of the CFD-3D scavenging and combustion simulations. The model layout is shown in Fig. 13.

A comparison between CFD-1D simulation and experiments is presented in the following figures. The operating conditions are: wide open throttle, injection and ignition parameters set for maximum brake torque (MBT) and low cycle-to-cycle variation, exhaust system tuned at low engine speed.

Fig. 14 shows: volumetric efficiency, indicated mean effective pressure (considering an average cycle), brake torque, brake specific fuel consumption.

Fig. 15 presents the average pressure traces measured and calculated within the cylinder, at the previous operating conditions.

A satisfactory agreement may be observed for all the graphs presented in Figs. 14 and 15.

In order to confirm the physical soundness of the calibrated GT-Power model, another set of operating conditions is considered, without changing the model calibration. Injection and ignition parameters are modified in order to minimize brake specific fuel consumption. Again, simulation and experiments are compared finding an excellent agreement, see Fig. 16.

6. Development of the prototype

From all the comparisons between simulation and experiments it can be concluded that the calibrated model of GT-Power is able to predict the influence of further modifications to the prototype.

In particular, a new version of the engine, featuring an electric supercharger, in place of the previous piston pump, is investigated. The scavenging and combustion systems remain the same.

Some drawings of the new engine are presented in Fig. 17. The cut-away view shows the main peculiarities of this 2-stroke range-extender: the lubrication system, as in a standard 4-stroke; the roots blower driven by an electric motor; a patented rotary valve, revving at the same speed of the crankshaft, controlling a set of auxiliary inlet ports; the gasoline direct injection system; the piston controlled ports, as in motorcycle engines.

The advantages expected from this evolution, in comparison to the previous prototype, are: (1) no need of valves to control the flow entering and leaving the piston pump, thus better reliability; (2) simple and efficient load control, through the speed of the electric supercharger (lower speeds correspond to lower airflow rates, without throttling losses); (3) easier blow-by control (no need of specific piston rings in the pump, to limit the oil passage from sump to cylinders); (4) more compact dimensions; (5) simple and efficient control of the internal EGR rate, through the speed of the electric supercharger (lower speeds correspond to higher EGR rates).

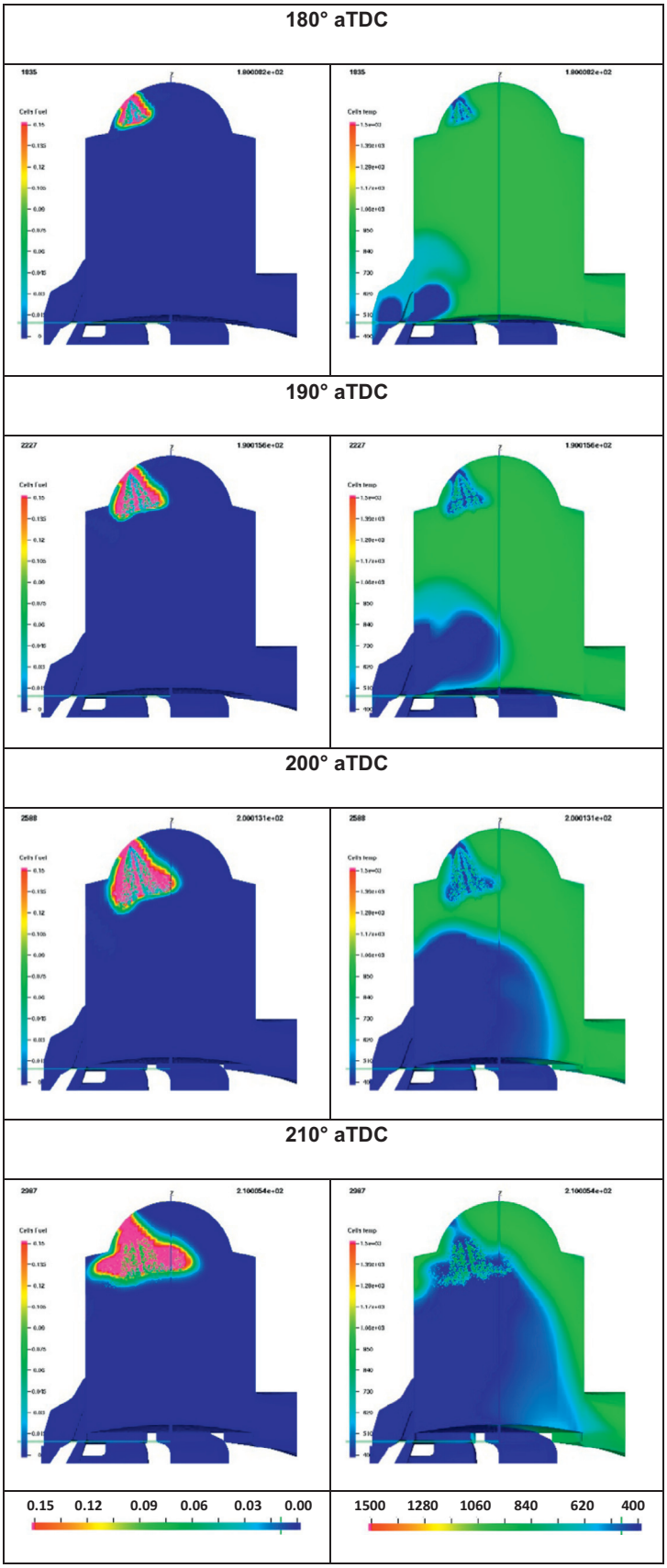

Fig. 9. Fuel concentration (left) and temperature (right) plotted on the symmetry plane at 180–190–200–210 cad after TDC. Full cycle simulation at 4500 rpm, full load, stoichiometric operations.

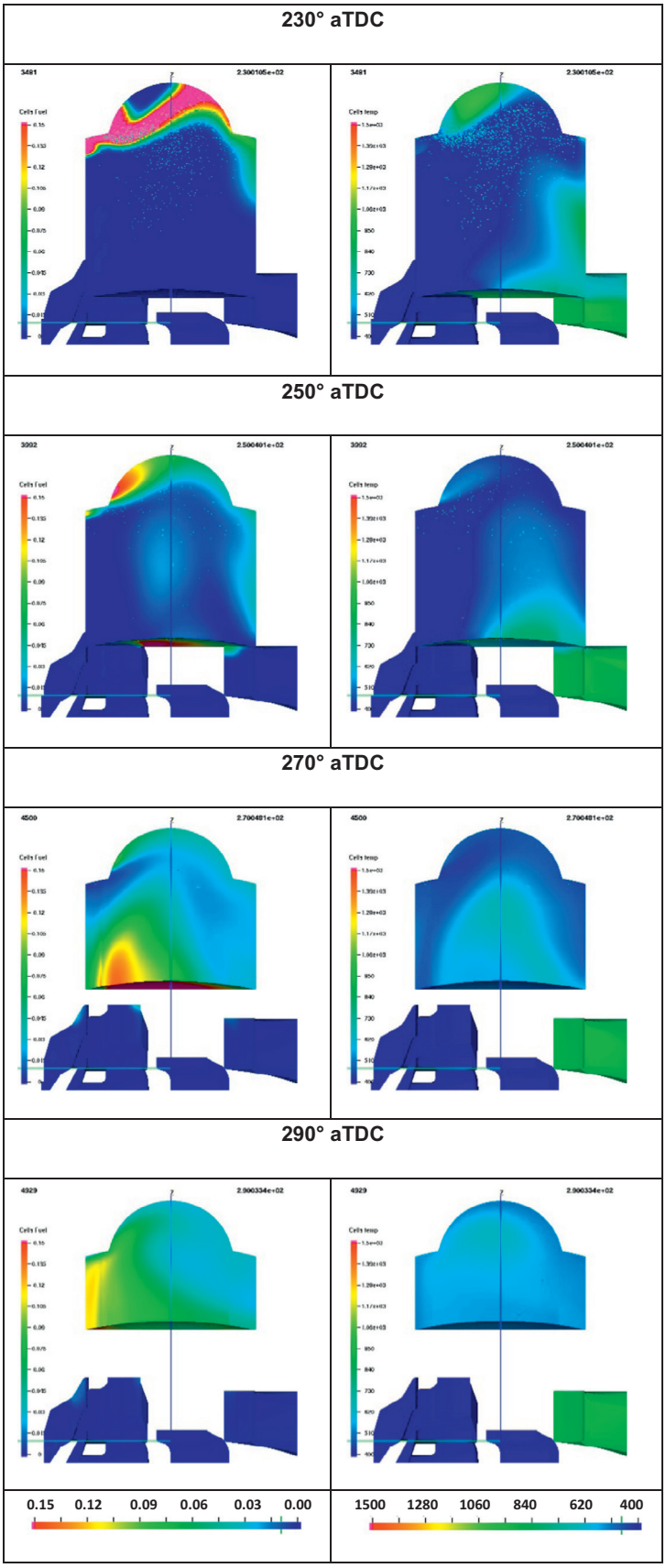

Fig. 10. Fuel concentration (left) and temperature (right) plotted on the symmetry plane at 230–250–270–290 cad after TDC. Full cycle simulation at 4500 rpm, full load, stoichiometric operations.

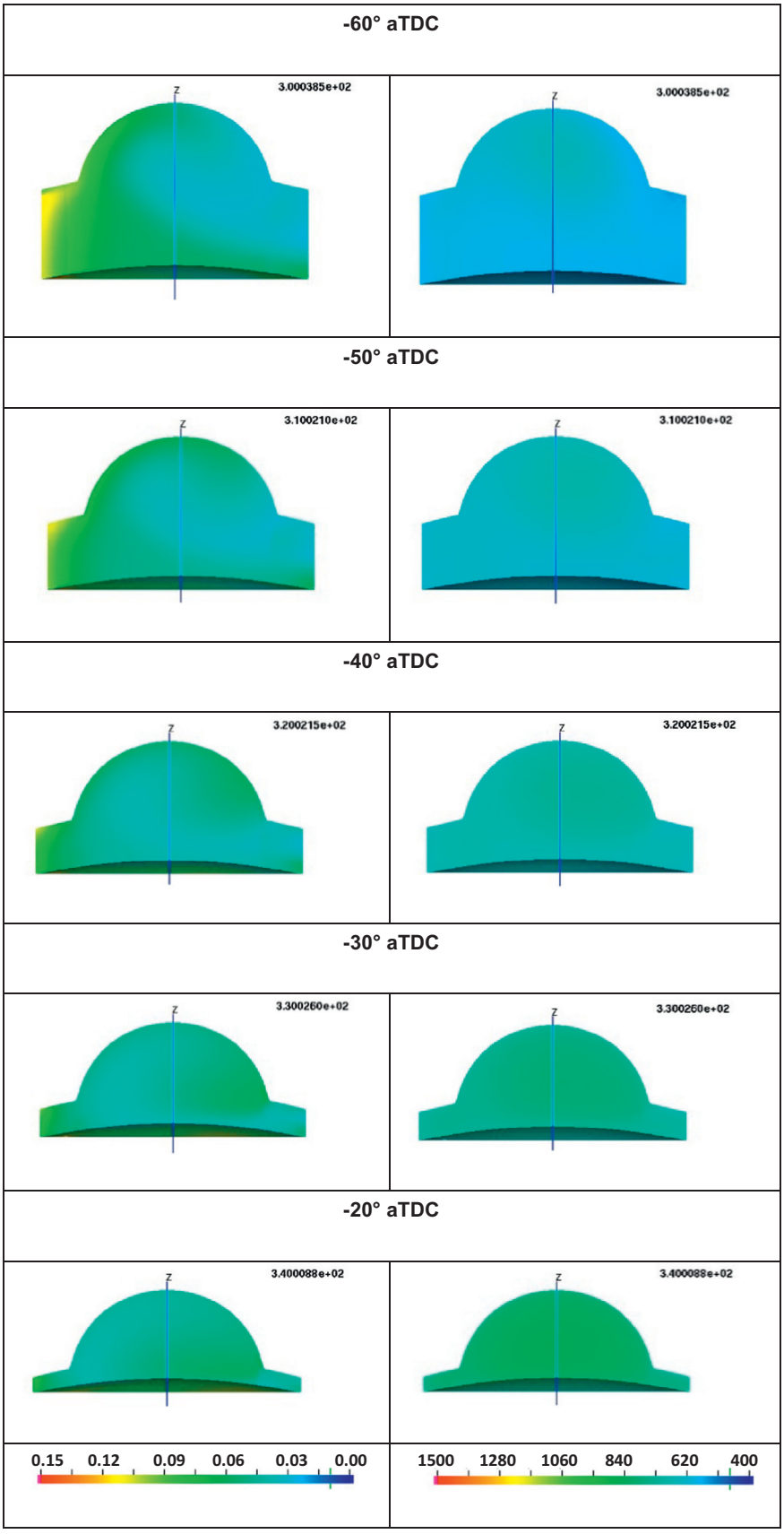

Fig. 11. Fuel concentration (left) and temperature (right) plotted on the symmetry plane at 300–310–320–330–340 cad after TDC. Full cycle simulation at 4500 rpm, full load, stoichiometric operations.

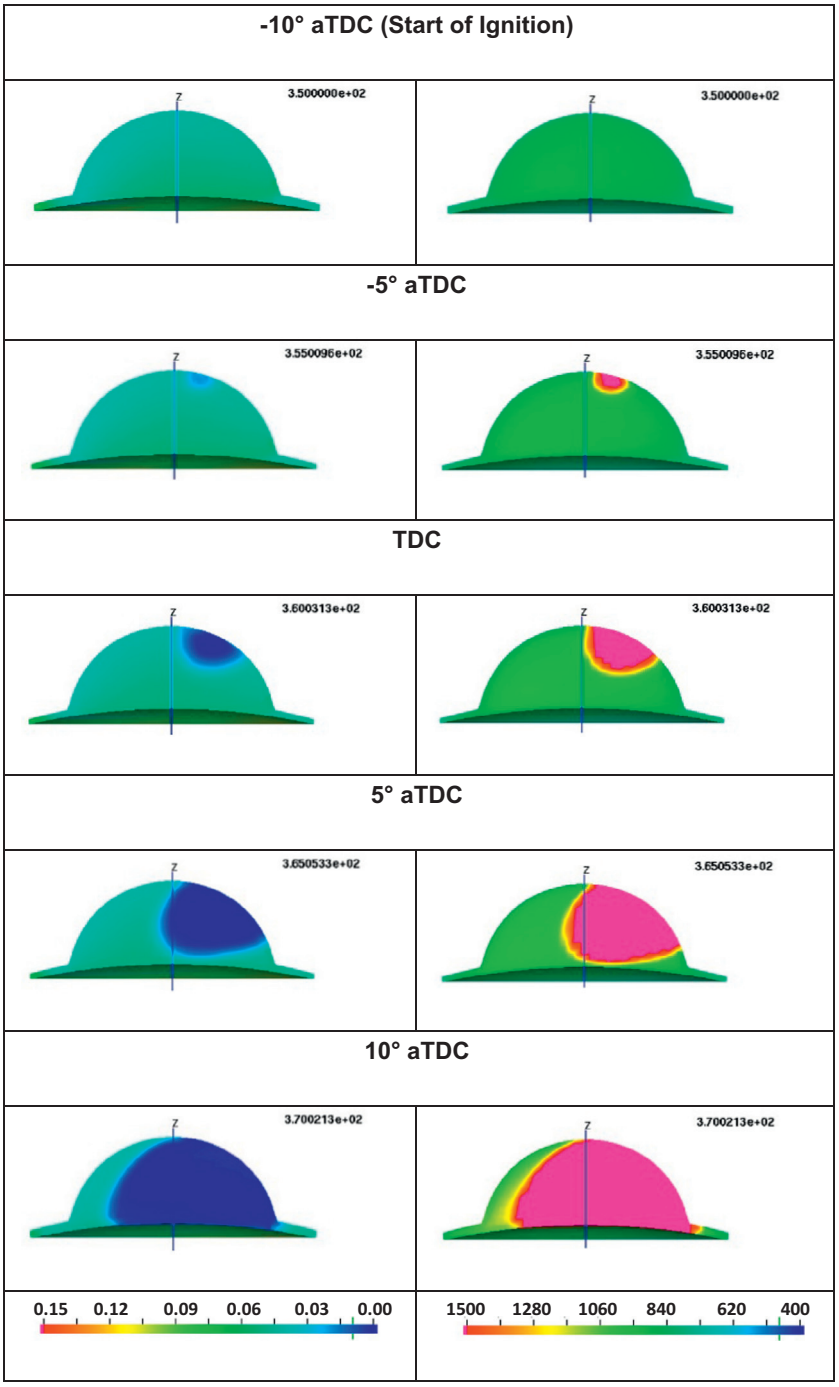

Fig. 12. Fuel concentration (left) and temperature (right) plotted on the symmetry plane at −10, −5, 0, 5 and 10 cad after TDC. Full cycle simulation at 4500 rpm, full load, stoichiometric operations.

6.1. Comparison with other 2-strokes

The proposed engine is strongly different from standard 2-stroke gasoline engines, as well as from other recent innovative 2-strokes.

The main differences from conventional small motorcycle engines are: direct fuel injection (no fuel losses through the exhaust ports, full control of the air-fuel ratio, capability to stratify the charge, then to run under lean conditions); lubrication as in 4-strokes (no oil dispersed in the exhaust flow, good lubrication at any operating condition); electric supercharger instead of the crankcase pump (much better control of the airflow, no need of a throttle valve); patented rotary valve (better scavenging control, enhanced quality of the process). As a result, reliability and fuel consumption are expected to be similar or even slightly better than in a standard 4-stroke engine, while all brake performance parameters are enhanced, thanks to the double cycle frequency. In terms of pollutant emissions, the proposed 2-stroke can adopt a 3-way catalyst, like a 4-stroke, being free from the typical issues affecting small motorcycle engines (dispersed oil, fuel burning in the exhaust pipes, etc.).

As far as the combustion and scavenging systems are concerned, the proposed engine is similar to the Orbital design [20], and also to the prototype developed by the University of Graz

Table 1
Experimental instrumentation and measurements accuracy.

Instrument	Parameter	Full scale	Accuracy
Apicom FR 400 BRV	Torque	900 Nm	0.2% FS
	Rotational speed	12.000 rpm	1 rpm
Endress + Hauser Proline t-mass 65F50	Combustion air flow rate	704 Nm^3/h	1.5% of reading
Flomec 0M004	Fuel consumption	36 liter/h	1% of reading
Kistler 6113B Measuring spark plug	In-cylinder pressure	200 bar	Linearity < 0.5% FSO
			Sensitivity drift < 1% of reading

[19]. In all the cases, both scavenge and exhaust ports are controlled by the piston, the combustion chamber has a spherical shape with the spark plug on the top, and the air-fuel mixing process is promoted by a single strong tumble vortex, generated by the flow entering the cylinder through the scavenge ports and deflected by the cylinder liner and head (loop scavenging). However, both the Orbital and the Graz engine feature a crankcase pump, with a reed valve controlling the inlet port. This solution is certainly compact and cheap, but it cannot prevent some lubricant oil to enter the cylinder and then go at the exhaust. Moreover, reliability of reed valves is generally poor. Conversely, the design proposed in this study, with a large oil sump, completely cancels these issues. Also the injection systems are different: the Graz engine adopts two low pressure injectors, the Orbital engine has got a patented air assisted injector, whereas the proposed engine uses a commercial GDI system by Magneti Marelli. This off-the-shelf solution is less expensive than an air assisted injector, and does not need the related complex and cumbersome circuit for delivering the secondary air. In comparison to the Graz low pressure fuel system, the proposed one is more expensive, but it has got enhanced capabilities: better fuel atomization, thanks to the much higher pressure (200 bar versus 5 bar), better charge stratification (injector and spark plug are very close).

Brunel University is studying a GDI 2-stroke engine, with piston controlled scavenge ports and exhaust poppet valves (named BUSDIG, [46]). Even if the details of the combustion system have not been disclosed at the moment of writing this paper (Spring 2017), this engine is clearly different from the proposed one. On the one hand, the presence of exhaust valve enables an efficient uniflow scavenging process; on the other hand, the valves need an actuation system, with ensuing higher pressure and friction losses, and they do not allow a free design of the combustion chamber. The lubrication system should be identical.

Brunel is also studying another 2-stroke concept [12], using the poppet valves of a 4-stroke 4-valve engine to control the scavenging process, as previously done by Toyota many years ago [47]. Again, the presence of poppet valves yields pros and cons; in the authors' opinion, a valve-less engine as the one shown in Fig. 17 is more suitable for range extender applications.

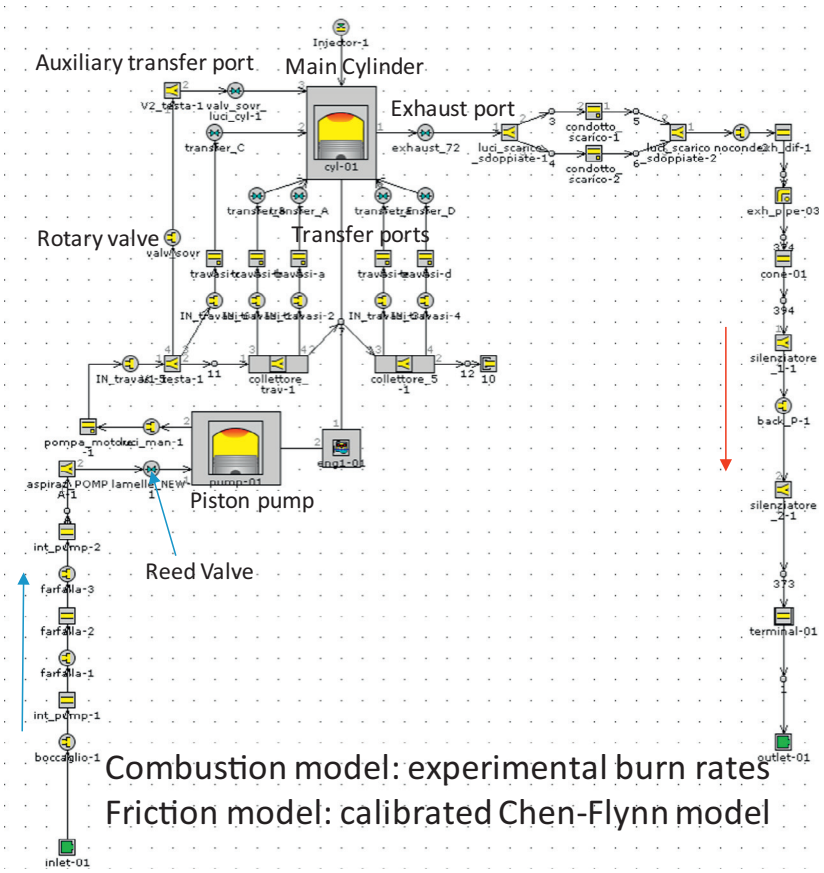

Fig. 13. Sketch of the GT-Power model of the prototype.

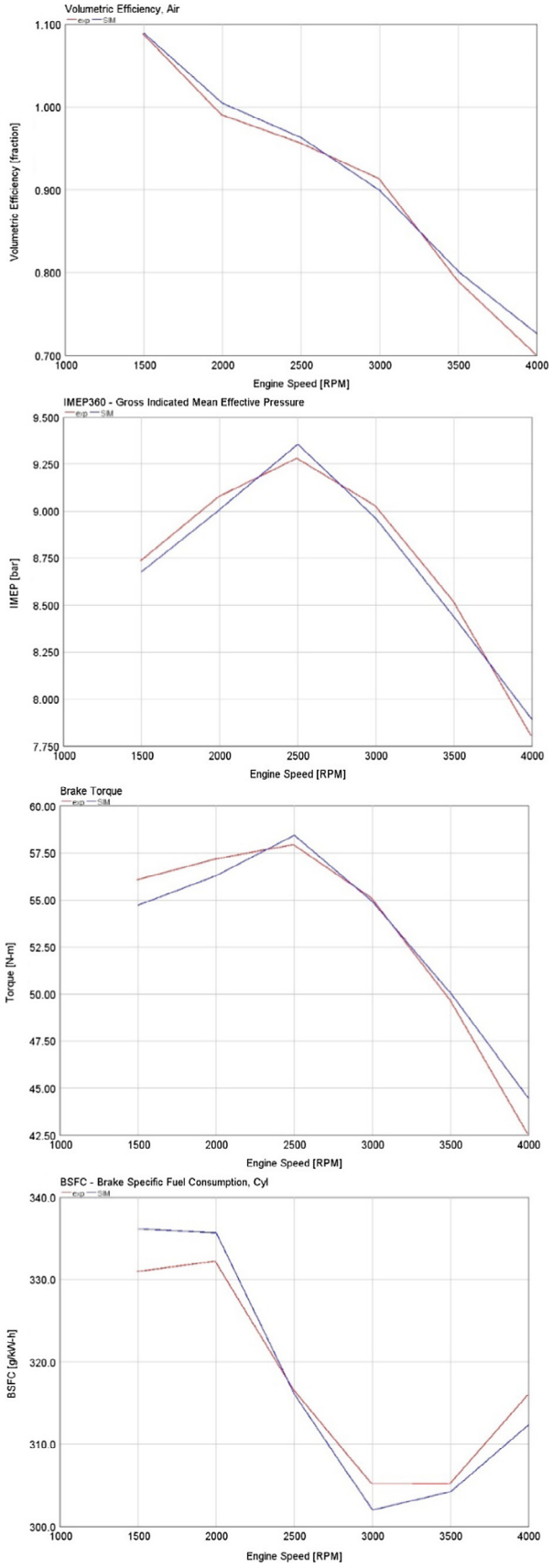

Fig. 14. Comparison between experimental and simulation results (GT-Power).

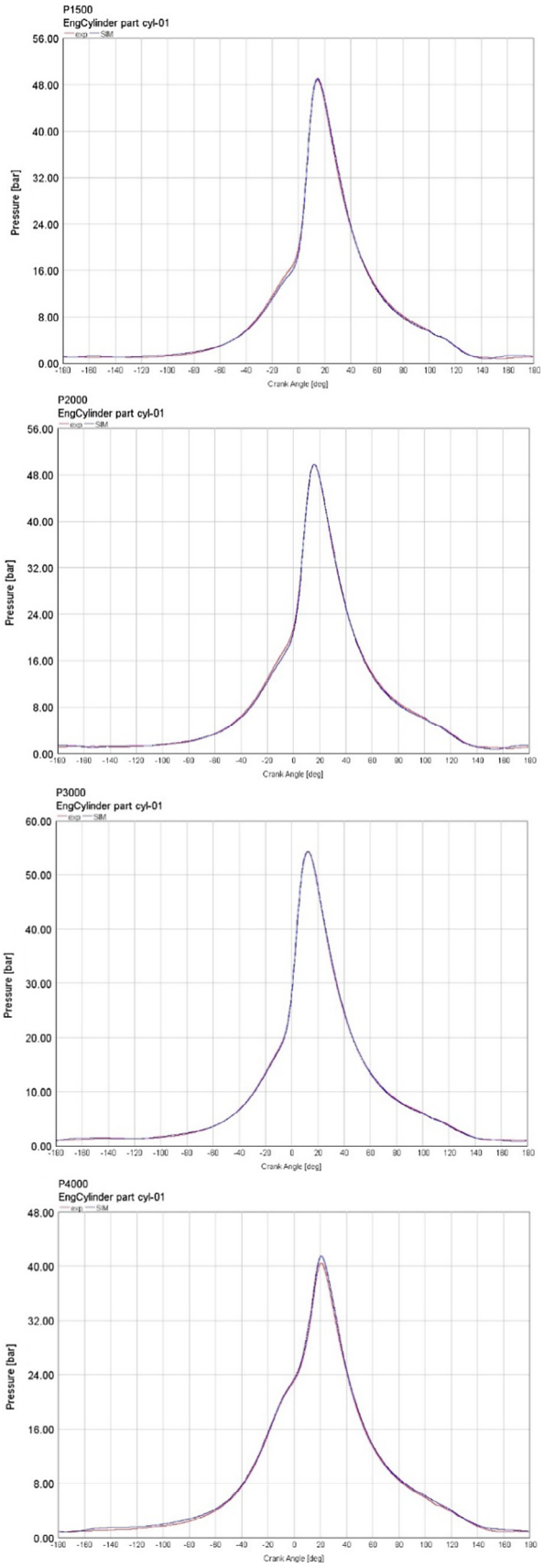

Fig. 15. Pressure traces measured and calculated at 1500, 2000, 3000 and 4000 rpm, full load.

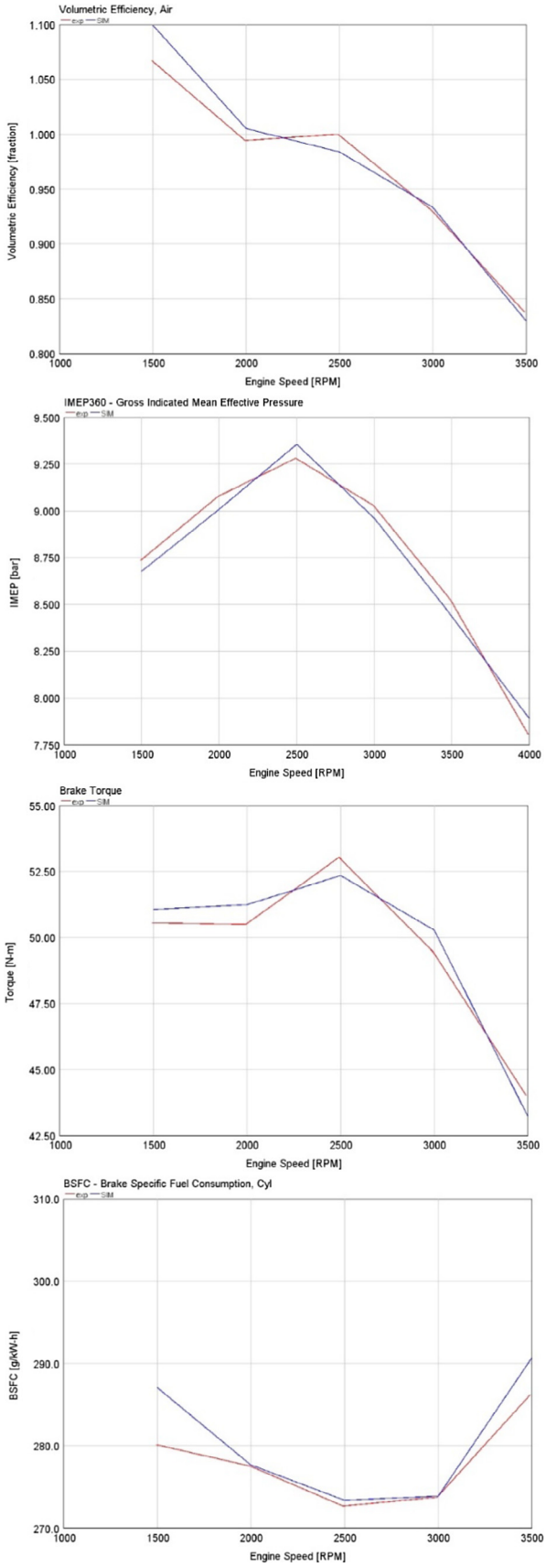

Fig. 16. Comparison between experiments and GT-Power simulation considering best efficiency operating conditions.

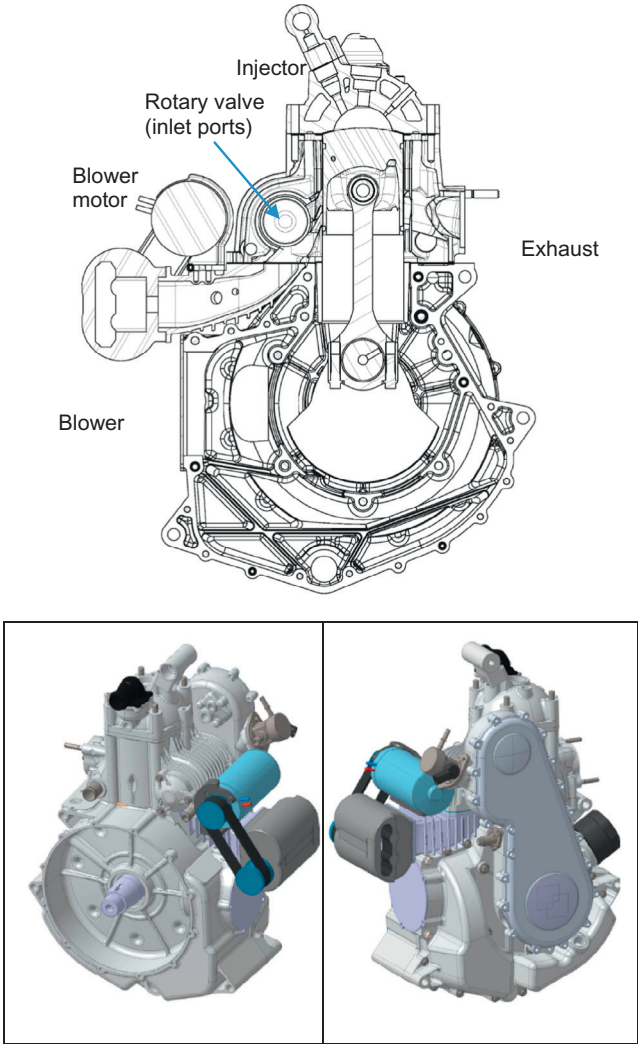

Fig. 17. The new 2-Stroke GDI engine.

Another recent interesting proposition is the Opposed Piston two stroke GDI engine, described in [48]. The engine features a single cylinder, with two pistons and two crankshafts. The single combustion chamber is formed by the pistons crown and the cylinder liner. Two spark plugs and one injector are installed in the middle of the cylinder. This design, known before the second world war, has got an excellent thermal efficiency [23], and it is able to generate an efficient uniflow scavenging without using poppet valves [49,50]. In comparison to the design shown in Fig. 17, the only downsides seem to be the double crankshaft, and the constraints on the shape of the combustion chamber, which can be an obstacle to achieve a proper stratification of the charge.

The engine concept more similar to the proposed one is that developed by the "Omnivore" project [21,22]. The research engine reviewed in the reference papers basically differs only for the use of both a valve to control the flow through the exhaust port, and a variable compression ratio mechanism in the cylinder head. This approach permits to operate more easily in HCCI mode, but it requires a quite cumbersome mechanical system, that does not appear to be suitable for range extender applications.

6.2. The reference 4-stroke engine

In order to put the calculated 2-stroke engine performance into perspective, a comparison is made with a correspondent 4-Stroke engine, developed by the authors. Obviously, the numerical results obtained for each engine type derive from the same set of constraints and goals.

Being the design of a 4-stroke range extender previously discussed by the authors [30], only the fundamental aspects will be reviewed here.

Because of the cost constraints, the most suitable technology appears to be a simple PFI 2-valve combustion system, with in-block camshaft and pushrods. The "antiquated" push rod technology bears no restrictions to the functionality of the engine, as high engine speeds are not desired due to NVH considerations. Conversely, the dimensions of the engine head may be reduced, in comparison to a conventional overhead camshaft.

The displacement resulting from the combination of the performance target and the choice of valves is about 0.75 l. With such a capacity, the number of cylinders must be no less than 2, in order to adopt conventional components. As far as the cylinder lay-out is concerned, a V-90° design appears better than a 2 in-line, because of the possibility to fully balance the first order mass forces by means of counter-weights on the crankshaft, instead of installing a balancer shaft, that causes additional parasitic losses. Regarding its space requirements, a V-90° concept with a disc-shaped generator directly flanged to the crankshaft is also attractive. The final outcome of the 4-S range extender optimization is reviewed in Table 2.

7. 2-S engine calibration

The main design targets and constraints considered for the two-stroke engine (as well as for the reference 4-Stroke) are listed below:

- 30 kW at 4500 rpm or lower speed
- Maximum combustion pressure: 80 bar
- Maximum Sound Pressure Level (SPL) measured at 0.5 m from the exhaust tailpipe (at 45°): 95 dB (A)
- Maximum temperature at the catalyst inlet: 800 °C
- No knocking

The limitation of in-cylinder pressure is a fundamental key for achieving a light design, while the control of the maximum pressure gradient and of the SPL are basic NVH requirements, set upon experience. Finally, the catalyst maximum temperature inlet is set to guarantee the reliability of the after-treatment system.

As already mentioned, the scavenging and combustion systems are basically the same of the tested prototype, so that the numerical analysis (by GT-Power) was focused on the supercharger set-up, as well as on the optimization of port timings (the height of the ports is adjusted to match the new type of scavenging pump).

Table 2
Main features of the reference 4-S range extender [25].

Engine type	V2 (90°), PFI, 2-valve
Engine bore × stroke [mm]	77 × 81
Engine displacement [cm^3]	750
Engine compression ratio (effective)	11:1
Intake valve seat diameter × max. lift [mm]	36 × 10
Exhaust valve seat diameter × max. lift [mm]	28 × 8.5
Intake valve opening/closing [CA° before DC]	21/−41
Exhaust valve opening/closing [CA° before DC]	51/−11
Estimated weight (w/o intake exhaust systems) [kg]	50

Table 3
Main features of the new 2-stroke range extender.

Engine bore × stroke [mm]	84 × 90
Engine displacement [cm^3]	499
Engine compression ratio (geometric)	16:1
Engine compression ratio (effective)	11.8:1
Supercharger displacement [cm^3]	346
Exhaust port opening/closing [CA° before BDC]	80/−80
Transfer port opening/closing [CA° before BDC]	40/−40
Auxiliary port opening [CA°. before BDC]	32
Auxiliary port closing [CA°. after BDC]	72

The numerical models employed in the study, presented in [20], are able to predict knocking occurrence, and the combustion parameters are set in order to avoid this phenomenon. The main features of the optimized engine are presented in Table 3.

The most important parameter for engine calibration is the speed of the supercharger. In order to assess its influence, a CFD-

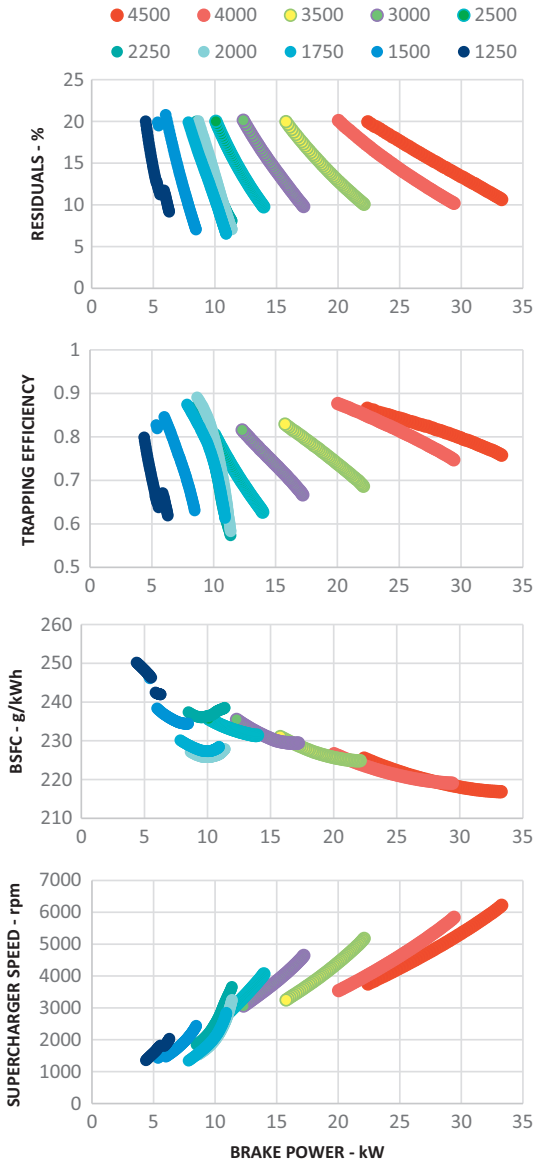

Fig. 18. Influence of supercharger speed on brake power, trapping efficiency, residuals and bsfc, at different engine speeds (from 1250 to 4500 rpm). CFD-1D Simulation results at wide open throttle, stoichiometric conditions within the cylinder.

1D engine simulation was run, considering some constant engine speeds (from 1250 to 4500 rpm), and a homogeneous stoichiometric combustion within the cylinder. The flow through the supercharger is un-throttled (wide open valve).

The main results of this analysis are presented in Fig. 18. It may be noticed that the amount of residual gas is limited to 15–25% (depending on engine speed), in order to avoid high cycle-by-cycle variations. This threshold was defined on the basis of the experimental results on the prototype, featuring an almost identical combustion system.

Fig. 2 shows that, as the supercharger velocity goes down, delivery ratio and brake power decrease, while trapping efficiency, brake specific fuel consumption and the amount of residual gas increase. As far as fuel efficiency is concerned, also engine speed plays an important role: as it increases, brake specific fuel consumption tends to decrease.

The trends of Fig. 18 can be explained by the following considerations.

- The delivered mass flow rate is almost proportional to supercharger speed, except at a few operating conditions, for the presence of specific dynamic effects in the tuned exhaust system.
- As the delivery ratio decreases, less air tends to leave the cylinder, and more residuals remain trapped with the fresh charge.
- Despite some recovery of trapping efficiency, a reduction of delivered air generally yields a decrease of trapped charge, thus a reduction of brake power.
- For a given engine speed, the best efficiency is reached at the maximum torque, simply because the friction and pumping losses have a lower weight, in comparison to the brake output.
- At full load, the best efficiency is reached at maximum engine speed, because the specific flow-dynamic tuning, aimed to achieve the maximum power rate.

8. Comparison between 2S and 4S

The most interesting operations for a range extender are the ones minimizing fuel consumption while complying with the most stringent emissions limits. For the 4-Stroke engine, this criterion reduces the operating range to full throttle operations and relative air-to-fuel ratio equal to 1. An exception may occur when it is not possible to keep the throttle wide open, along with stoichiometric mixture, for knocking issues: in this case, it will be considered the maximum throttle opening angle corresponding to Lambda 1.

For the 2-Stroke engine, the range of operating conditions is limited by two further constraints: (1) residuals within the cylinder as high as possible (limit: cycle-by-cycle variation); (2) trapping efficiency higher than 80%. These two constraints should avoid the installation of an expensive De-NOx after-treatment system, since the internal EGR should reduce NOx formation, while the catalyst should work at acceptable levels of efficiency.

Some characteristics of both engines are plotted as a function of the delivered brake power. In particular, the parameters selected for the comparison are: (1) engine speed; (2) brake specific fuel consumption; (3) trapping efficiency (4) Fraction of residual gas in the trapped charge; (5) airflow rate; (6) maximum rate of pressure rise; (7) gross indicated mean effective pressure; (8) total heat rejected by the engine; (9) pumping efficiency; (10) mechanical efficiency (see Figs. 19–28).

Engine speed: The 4-S engine can reach any target power at a velocity lower, the maximum gap is at 22 kW (1500 rpm), the minimum at 30 kW (100 rpm). This is an advantage in terms of NVH for the 4-S unit.

BSFC/brake efficiency: The advantage of the new 2-S engine is quite evident, in particular at high power rates: on average, it saves about 6% of fuel, and the maximum benefit is 10% at high power rates. The main reason for this superior efficiency is the indicated cycle, where a larger fraction of the heat released by combustion is converted into work.

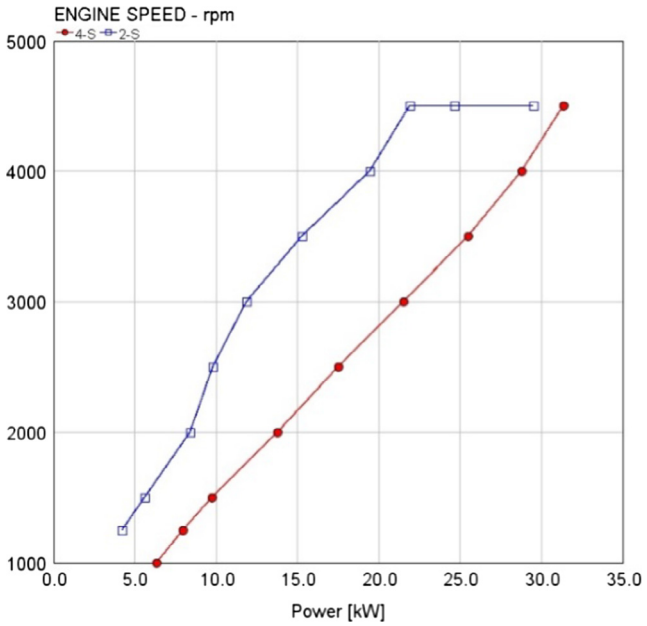

Fig. 19. Comparison between the new 2-S GDI engine and a reference 4-S in terms of engine speed.

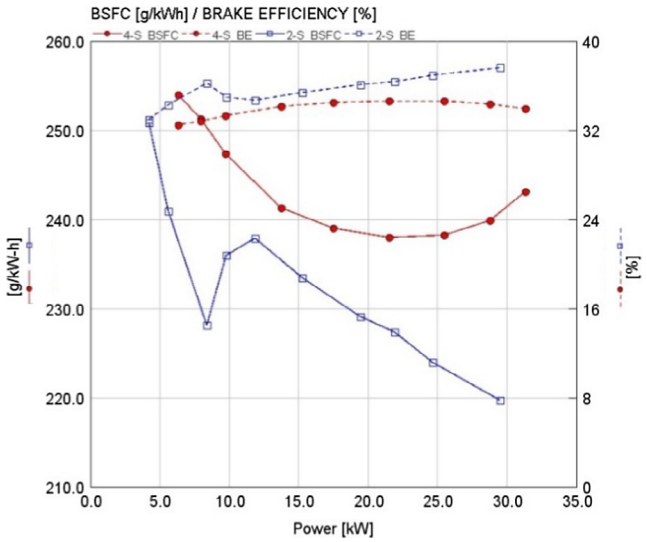

Fig. 20. Comparison between the new 2-S GDI engine and a reference 4-S in terms of brake specific fuel consumption and brake efficiency.

Gross indicated efficiency: The higher efficiency of the 2-Stroke indicated cycle is particularly visible at medium-low power rates, where heat losses have more weight in the energy balance. Also the high geometric compression ratio helps the efficiency of the 2-stroke cycle, even if this aspect is partly compensated by the early exhaust opening.

Rejected heat: In the 4-S unit, the maximum rate of heat rejected by the engine (from both cylinder heat transfer and friction losses) is about 20% higher. The reasons are: (1) the duration of a 4S stroke cycle is double, thus hot gases remain for a longer time within the cylinder; (2) the power associated to mechanical friction is higher

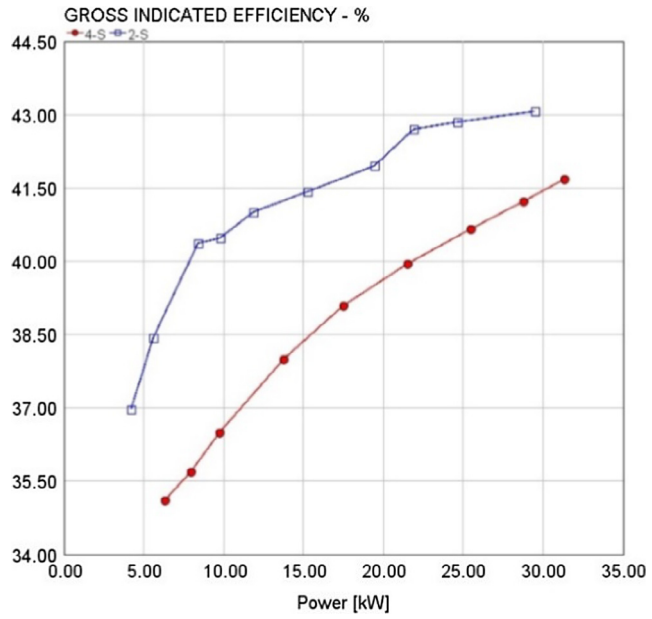

Fig. 21. Comparison between the new 2-S GDI engine and a reference 4-S in terms of gross indicated efficiency.

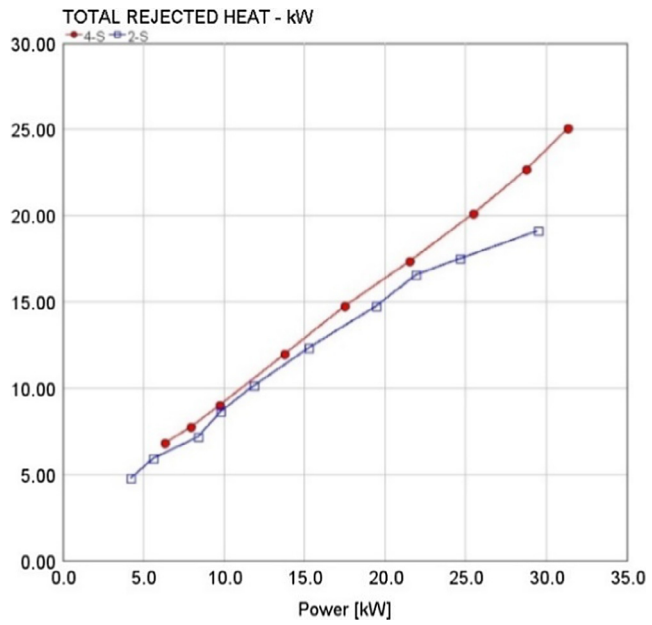

Fig. 22. Comparison between the new 2-S GDI engine and a reference 4-S in terms of heat rejected by the engine.

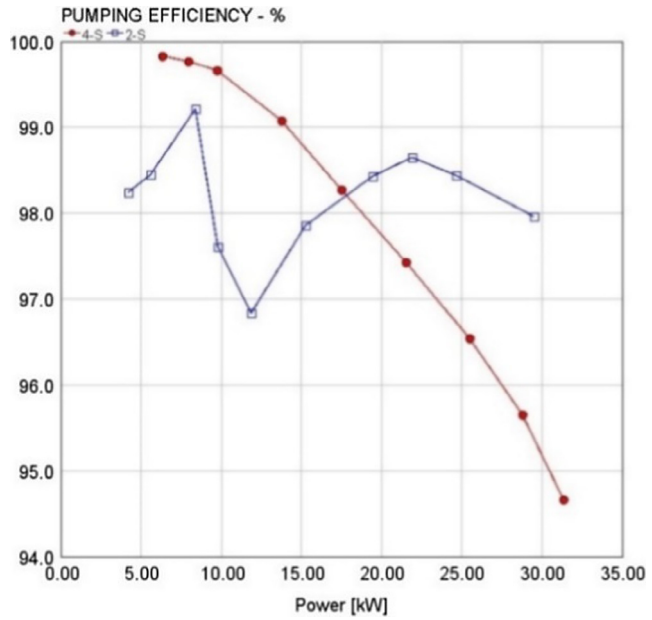

Fig. 23. Comparison between the new 2-S GDI engine and a reference 4-S in terms of pumping efficiency.

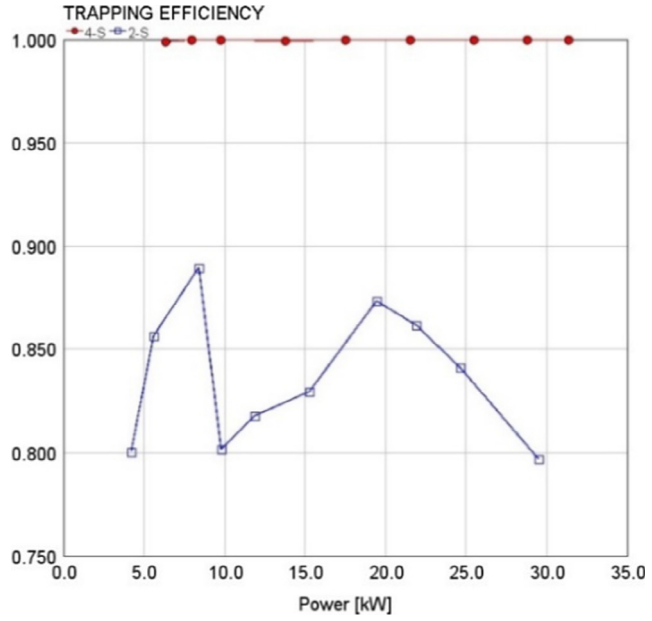

Fig. 24. Comparison between the new 2-S GDI engine and a reference 4-S in terms of trapping efficiency.

in the 4-S engine, because of the valve-train and for the larger total displacement; (3) the total surface of the combustion chambers is larger in the 4-S engine (two cylinders); (4) combustion temperature is lower in the 2-Stroke engine, for the large presence of residuals. A lower rejected heat allows the designer to reduce the overall dimensions of the heat exchangers, an interesting aspect in favor of the 2-S powertrain.

Pumping efficiency: This graph demonstrates that the electric supercharger is a very efficient solution, in particular at high power rates: here, the energy lost for driving the blower is 3% less than the correspondent pumping work in the 4-Stroke engine. The maximum power required by the supercharger is 0.62 kW, for a brake power of 30 kW.

Trapping efficiency: Thanks to the supercharger control, the 2-S engine shows relatively high values of trapping efficiency (>80%). This parameter is fundamental to avoid that the presence of Oxygen in the exhaust flow freezes the reduction reactions within the catalyst.

Residuals: In order to compensate the lower efficiency of the catalyst, the trapped charge within the 2-S engine is diluted with a relatively high content of residuals (up to 22%).

Airflow: For delivering the same power rating, the 2-Stroke engine requires up to 20% of additional air, due to the lower trapping efficiency.

Max. rate of pressure rise: Combustion is quite similar in the two engines, as demonstrated by the in-cylinder maximum rate of

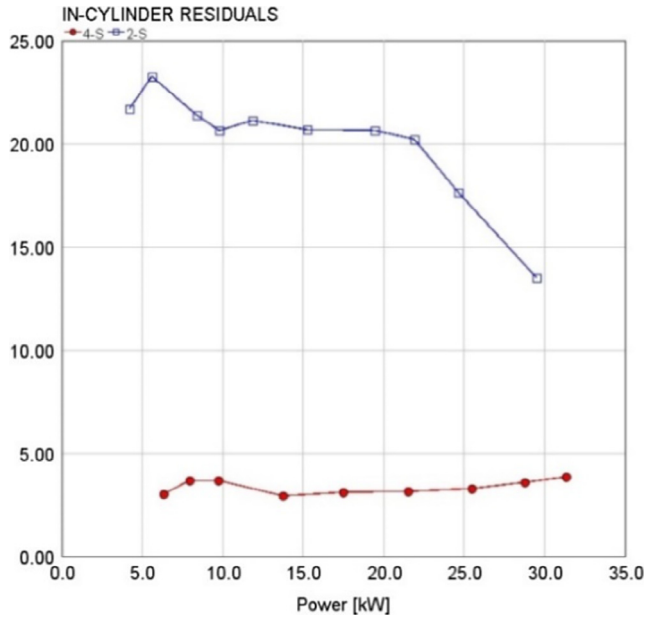

Fig. 25. Comparison between the new 2-S GDI engine and a reference 4-S in terms of in-cylinder residuals.

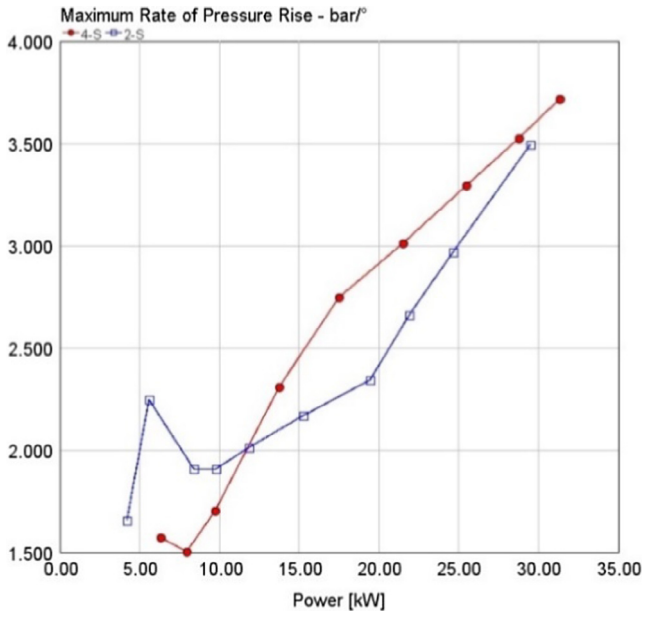

Fig. 27. Comparison between the new 2-S GDI engine and a reference 4-S in terms of engine maximum rate of pressure rise.

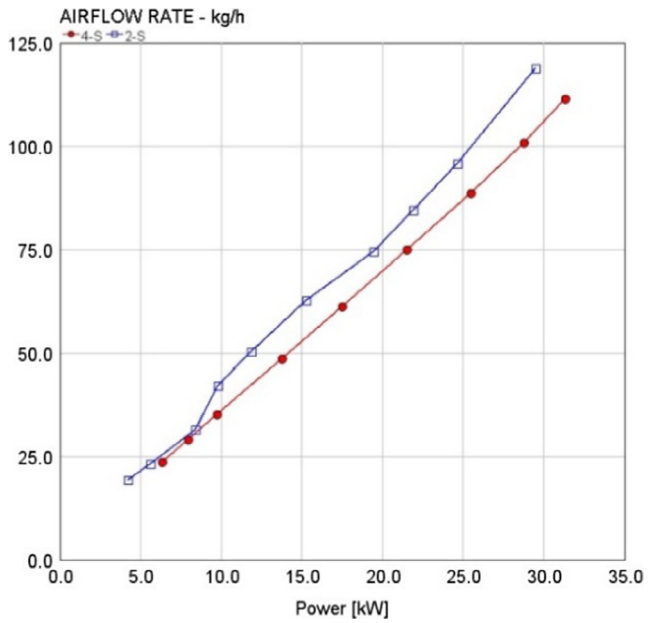

Fig. 26. Comparison between the new 2-S GDI engine and a reference 4-S in terms of delivered airflow rate.

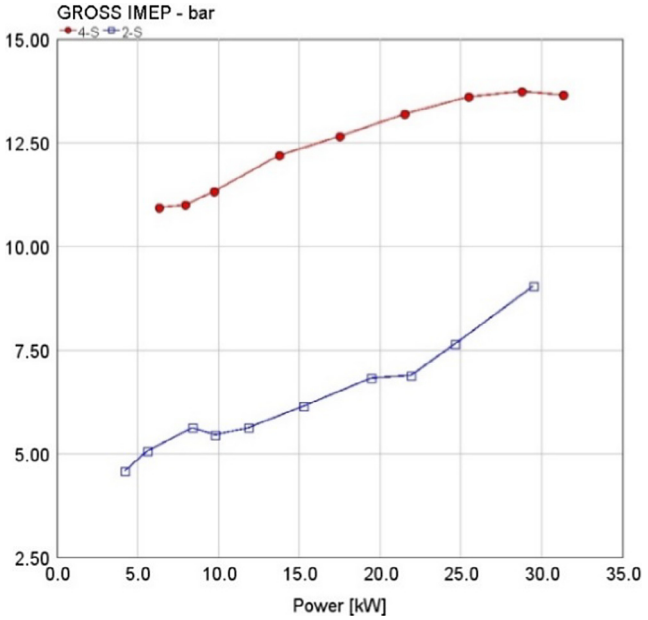

Fig. 28. Comparison between the new 2-S GDI engine and a reference 4-S in terms of gross IMEP.

pressure rise. The 2-S engine seems to have a slight advantage in terms of combustion noise at medium-high power rates, while the contrary occurs at low speeds. The outcome is not particularly surprising, considering that the spark advance is set in the same way (maximum brake torque), and that the 2-S engine can compensate the high internal EGR with a higher level of turbulence, and with the support of direct injection.

Gross IMEP: The specific work done in the compression-expansion stroke is about 5 bar higher in the 4-S engine: as a result, also the thermal and mechanical loads on the cylinder components are higher. This advantage for the 2-S engine may be exploited in many ways: weight reduction, cost reduction (adopting less expensive manufacturing technologies), increase of maintenance intervals.

For the new 2-S loop scavenged SI engine, an accurate estimation of overall dimensions and weight can be made, on the basis of the CAD model (shown in Fig. 29), as well as on the experience gained from the physical prototype.

Mounting the 2-S engine as illustrated in Fig. 29, and considering also the electric generator, the overall dimensions are: in the plane orthogonal to the crankshaft axis a height of 607 mm and a width of 467 mm; along the crankshaft, a length of 303 mm. The estimated weight of the prototype is 33 kg (2 kg less the current PRIMAVIS prototype). It should be considered that the proposed

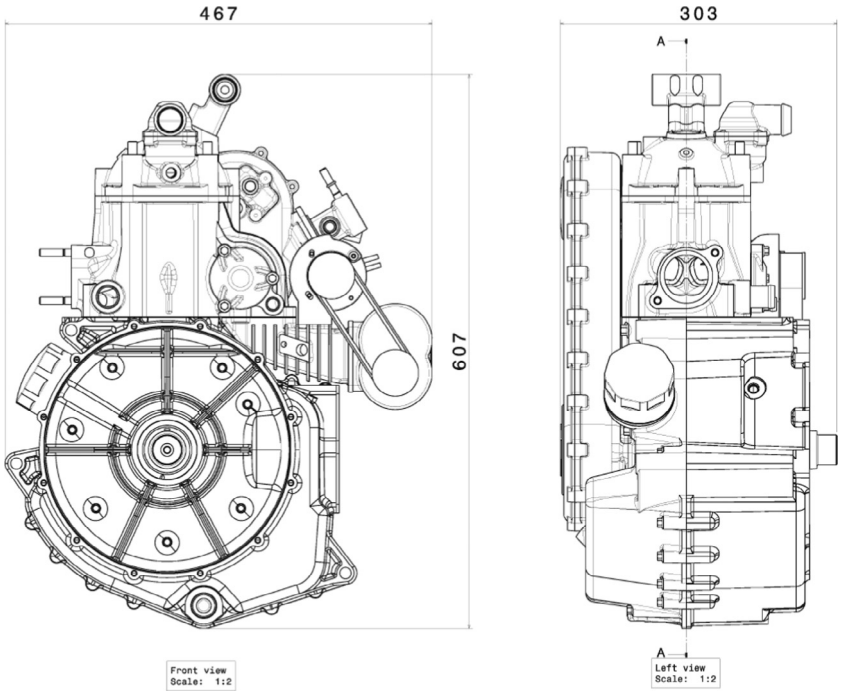

Fig. 29. Drawings of the proposed 2-Stroke range extender.

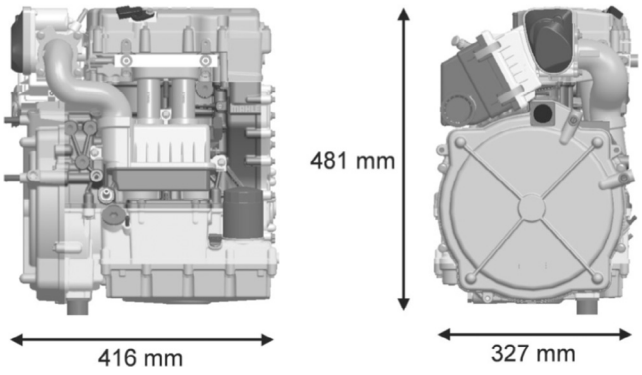

Fig. 30. Overall dimensions of the 4-Stroke 30 kW range-extender by Mahle [5].

engine is at an early stage of development, thus further improvements are expected in terms of compactness and weight.

In order to make a qualitative comparison between the proposed 2-stroke engine and a 4-stroke one, the Mahle range extender may be considered. The overall dimensions of this engine are shown in Fig. 30, while the declared weight, without electric generator, is 50 kg [5]. Overall dimensions are comparable with the two stroke unit, but the weight is 50% higher than the latter.

9. Summary and conclusions

The paper reviews the design and experimental development of an original 2-Stroke GDI range extender engine rated at 30 kW, 4500 rpm.

The proposed 2-Stroke engine is the evolution of a prototype built by PRIMAVIS and tested at the University of Modena and Reggio Emilia. The experimental campaign reveals that the combustion, injection and scavenging systems, developed with the support of CFD 1D and 3D simulations, work as predicted by these tools. However, the air metering system needs some modifications, in order to fix some reliability issues: therefore, the piston pump is replaced by a small electric supercharger (maximum power required by the motor: 0.62 kW). The new configuration is studied by means of 1D engine simulations, using experimentally calibrated models.

The following advantages are found for the proposed 2-S engine, in comparison to a reference 4-S (theoretically developed by the authors, considering the same constraints and goals):

- lower weight (−35%)
- lower thermal and mechanical loads within the cylinder (−40%, on average), thus NVH advantages;
- lower rejected heat −18%)
- better brake efficiency for all the power rates (up to +10%, +6% on average)
- wide margins for further combustion improvements, exploiting the potential of direct injection, and the freedom concerning the combustion chamber geometry.

The main issues of the 2-Stroke engine, in comparison to a 4-S are:

- lower efficiency of the 3-way catalyst, for the reduction of NOx; it must be compensated by diluting the charge with residuals;
- lower torque: for reaching the same power the engine must run up to 1500 rpm faster, except at peak power;
- complex set-up of the injection parameters, a strong support from CFD-3D simulation is required;
- the penalty for a poor air-fuel mixing could be a particulate filter, as on the next GDI 4-S engines;
- crankshaft balance less effective than in a V2 engine.

The next step of the project will be an experimental campaign on the modified prototype, including the measure of pollutant emissions.

Acknowledgments

Ing. Gabriele Rizzo and Ing. Davide Mollo of BRC Racing Team are gratefully acknowledged for their fundamental support to the experimental activities.

Gamma Technologies is gratefully acknowledged for granting the academic license of GT-Power to the University of Modena and Reggio Emilia.

References

[1] Li J, Wang Y, Chen J, Zhang X. Study on energy management strategy and dynamic modeling for auxiliary power units in range-extended electric vehicles. Appl Energy 2016.

[2] Doucette RT, McCulloch MD. Modeling the prospects of plug-in hybrid electric vehicles to reduce CO_2 emissions. Appl Energy 2011;88(7):2315–23.

[3] Turner J, Blake D, Moore J, Burke P, et al. The lotus range extender engine. SAE Int J Engines 2010;3(2):318–51. http://dx.doi.org/10.4271/2010-01-2208.

[4] GETRAG website. GETRAG boosted range extender 2RET300. Press Release by GETRAG. Available on: http://www.getrag.com/iaa/fileadmin/content/pdf/products/engl/Press_information_2RET300.pdf.

[5] Warth M. Mahle product information 09/2013. Document available at: http://www.mahle-powertrain.com/C1257126002DFC22/vwContentByUNID/7BD528F92F833F5BC12578D1004AA089/$FILE/09-2013%20Compact_Range_Extender_Engine_EN.pdf. 09/2013.

[6] KSPG press release. Low-noise range extender dispels battery runtime angst. Available at: http://presse-center.kspg.de/no_cache/en/press-kits/pm-single-en/article/geraeuscharmer-range-extender-nimmt-reichweitenangst-1.html. 13/01/2014.

[7] Fraidl G, Beste F, Kapus P, Korman M et al. Challenges and solutions for range extenders - from concept considerations to practical experiences. SAE Technical Paper 2011-37-0019; 2011. http://dx.doi.org/10.4271/2011-37-0019.

[8] Fischer et al. Range extender module – enabler for electric mobility. ATZ Autotechnology, vol. 9. May 2009. pp. 40–46.

[9] Shah, Raja Mazuir Bin Raja Ahsan, McGordon, Andrew, Amor-Segan, Mark, Jennings P.A. Micro gas turbine range extender: validation techniques for automotive applications. In: 4th Hybrid Electric Vehicle Conference (HEVC 2013), London, United Kingdom, 6–7 Nov 2013. Published. In: HEVC 2013: 4th Hybrid and Electric Vehicles Conference.

[10] Hooper PR, Al-Shemmeri T, Goodwin MJ. Advanced modern low-emission two-stroke cycle engines. Proc Inst Mech Eng, Part D: J Automob Eng 2011;225:1531. http://dx.doi.org/10.1177/0954407011408649.

[11] Zhang Y, Zhao H. Investigation of combustion, performance and emission characteristics of 2-stroke and 4-stroke spark ignition and CAI/HCCI operations in a DI gasoline. Appl Energy 2014;130:244–255. ISSN 0306–2619. http://dx.doi.org/10.1016/j.apenergy.2014.05.036.

[12] Macklini Dalla Nora, Hua Zhao, High load performance and combustion analysis of a four-valve direct injection gasoline engine running in the two-stroke cycle. Appl Energy 2015;159:117–131. ISSN 0306–2619. http://dx.doi.org/10.1016/j.apenergy.2015.08.122.

[13] Zhang Y, Zhao H, Ojapah M, Cairns A. Experiment and analysis of a direct injection gasoline engine operating with 2-stroke and 4-stroke cycles of spark ignition and controlled auto-ignition combustion. SAE Technical Paper 2011-01-1774; 2011. http://dx.doi.org/10.4271/2011-01-1774.

[14] Gentili R, Frigo S. ATAC and GDI in a small two-stroke engine. SAE Technical Paper 1999-01-3273; 1999. http://dx.doi.org/10.4271/1999-01-3273.

[15] Zanforlin S, Gentili R. Stable fuel confinement in stratified charge GDI engines. In: ASME 2004 internal combustion engine division fall technical conference. American Society of Mechanical Engineers; 2004.

[16] Musu E, Frigo S, De Angelis F, Gentili R et al. Evolution of a small two-stroke engine with direct liquid injection and stratified charge. SAE Technical Paper 2006-32-0066; 2006. http://dx.doi.org/10.4271/2006-32-0066.

[17] Payri F, Galindo J, Climent H, Pastor J et al. Optimisation of the scavenging and injection processes of an air-assisted direct fuel injection 50 Cc. 2-Stroke S.I. Engine by means of modelling. SAE Technical Paper 2001-01-1814; 2001. http://dx.doi.org/10.4271/2001-01-1814.

[18] Ferrara G, Bellissima A, Doveri M, Balduzzi F. Development of a non-conventional two stroke small engine for scooter applications. SAE Int J Engines 2010;3(2):462–72. http://dx.doi.org/10.4271/2010-32-0016.

[19] Krimplstätter S, Winkler F, Oswald R, Abis A, Schögl O, Kirchberger R. Layout and development of a 300 cm 3 high performance 2S-LPDI engine. SAE Technical Paper 2015-32-0832; 2015.

[20] Houston R, Archer M, Moore M, Newmann R. Development of a durable emissions control system or an automotive two-stroke engine. SAE Technical Paper 960361; 1996. http://dx.doi.org/10.4271/960361.

[21] Turner J, Blundell D, Pearson R, Patel R, et al. Project omnivore: a variable compression ratio ATAC 2-stroke engine for ultra-wide-range HCCI operation on a variety of fuels. SAE Int J Engines 2010;3(1):938–55. http://dx.doi.org/10.4271/2010-01-1249.

[22] Blundell D, Turner J, Pearson R, Patel R et al. The omnivore wide-range auto-ignition engine: results to date using 98RON unleaded gasoline and E85 fuels. SAE Technical Paper 2010-01-0846; 2010. http://dx.doi.org/10.4271/2010-01-0846.

[23] Herold R, Wahl M, Regner G, Lemke J et al. Thermodynamic benefits of opposed-piston two-stroke engines. SAE Technical Paper 2011-01-2216; 2011. http://dx.doi.org/10.4271/2011-01-2216.

[24] Ricardo H, Hempson JGG. The high-speed internal combustion engine – fifth edition. Editor: London: Blackie & Son Limited; 1968.

[25] Heywood JB, Sher E. The two stroke cycle engine – its development, operation, and design. Taylor & Francis, Inc. ISBN 1-56032-831-2.

[26] Controlled Power Technologies website. CPT%20COBRA_4pp_APR2014_4print%20(2)-1.pdf. downloadable from http://www.cpowert.com/assets. January 18, 2017.

[27] Eaton website. http://www.eaton.com/Eaton/ProductsServices/Vehicle/Superchargers/EAVS-supercharger/index.htm#tabs-4. January 18, 2017.

[28] Mattarelli E, Rinaldini C, Agostinelli E. Comparison of supercharging concepts for SI engine downsizing. SAE Technical Paper 2016-01-1032; 2016. http://dx.doi.org/10.4271/2016-01-1032.

[29] Tran H, Richard B, Gray K, Bassett M. Developing a performance specification for an electric supercharger to satisfy a range of downsized gasoline engine applications. SAE Technical Paper 2016-01-1041; 2016. http://dx.doi.org/10.4271/2016-01-1041.

[30] King J, Barker L, Turner J, Martin J, SuperGen – a novel low costs electro-mechanical mild hybrid and boosting system for engine efficiency enhancements. SAE Technical Paper 2016-01-0682; 2016. http://dx.doi.org/10.4271/2016-01-0682.

[31] Mattarelli E, Rinaldini C, Baldini P. Modeling and experimental investigation of a 2-stroke GDI engine for range extender applications. SAE Technical Paper 2014-01-1672; 2014. http://dx.doi.org/10.4271/2014-01-1672.

[32] Mattarelli E, Rinaldini C, Cantore G, Agostinelli E. Comparison between 2 and 4-stroke engines for a 30 kW range extender. SAE Int J Alt Power 2015;4(1):67–87. http://dx.doi.org/10.4271/2014-32-0114.

[33] Mattarelli E, Rinaldini CA, Cantore G. CFD optimization of a 2-stroke range extender engine. Int J Automot Technol 2015;16(3):351–69.

[34] Mattarelli E, Rinaldini CA, Cantore G. Comparison between a diesel and a new 2-stroke GDI engine on a series hybrid passenger car. No. 2013-24-0085. SAE Technical Paper; 2013.

[35] Baldini P. 2-Stroke engine with low consumption and low emission. International Patent PCT/IT2010/000057, Publication N° WO/2011/101878, on August 25, 2011.

[36] Mattarelli E. Virtual design of a novel 2-Stroke HSDI diesel engine. Int J Engine Res. Professional Engineering Publishing, Issue of June 2009;10(No. 3) ISSN 1468–0874 pp. 175–193.

[37] Cantore G, Mattarelli E. A new concept for ultra-compact automotive HSDI diesel engines. SAE Technical Paper 2007-01-1253; 2007. http://dx.doi.org/10.4271/2007-01-1253.

[38] De Marco C, Mattarelli E, Paltrinieri F, Rinaldini C. A new combustion system for 2-Stroke HSDI diesel engines. SAE Technical Paper 2007-01-1255; 2007. http://dx.doi.org/10.4271/2007-01-1255.

[39] Mattarelli E, Fontanesi S, Gagliardi V, Malaguti S. Multidimensional cycle analysis on a novel 2-Stroke HSDI diesel engine. SAE Technical Paper 2007-01-0161; 2007. http://dx.doi.org/10.4271/2007-01-0161.

[40] Mattarelli E, Rinaldini C, Wilksch M. 2-Stroke high speed diesel engines for light aircraft. SAE Int J Engines 2011;4(2):2338–60. http://dx.doi.org/10.4271/2011-24-0089.

[41] Rinaldini C, Mattarelli E, Golovitchev V. CFD analyses on 2-Stroke high speed diesel engines. SAE Int J Engines 2011;4(2):2240–56. http://dx.doi.org/10.4271/2011-24-0016.

[42] Mattarelli E, Rinaldini C, Savioli T. Port design criteria for 2-Stroke loop scavenged engines. SAE Technical Paper 2016-01-0610; 2016. http://dx.doi.org/10.4271/2016-01-0610.

[43] Savioli T. CFD analysis of 2-Stroke engines. Energy Procedia 2015;81:723-731. ISSN 1876-6102. http://dx.doi.org/10.1016/j.egypro.2015.12.078. (http://www.sciencedirect.com/science/article/pii/S1876610215027277).

[44] Rinaldini CA, Mattarelli E, Savioli T, Cantore G, Garbero M, Bologna A. Performance, emission and combustion characteristics of a IDI engine running on waste plastic oil. Fuel 2016;183:292–303.

[45] Rinaldini CA, Mattarelli E, Magri M, Beraldi M. Experimental investigation on biodiesel from microalgae as fuel for diesel engines. SAE Technical Paper 2014-01-1386; 2014.

[46] Wang X, Ma J, Zhao H. Analysis of the effect of intake plenum design on the scavenging process in a 2-Stroke boosted uniflow scavenged direct injection gasoline (BUSDIG) engine. SAE Technical Paper 2017-01-1031; 2017. http://dx.doi.org/10.4271/2017-01-1031.

[47] Nomura K, Nakamura N. Development of a new two-stroke engine with poppet-valves: Toyota S-2 engine. A new generation of two-stroke engines for the future?. In: Duret P, editor. Proceedings of the international seminar held at IFP, Rueil-Malmaison, France, 29–30 November 1993. pp. 53–62.

[48] Ma Fu-Kang, Wang Jun, Feng Yao-Nan, Zhang Yan-Gang, Tie-Xiong Su, Zhang Yi, et al. Parameter optimization on the uniflow scavenging system of an OP2S-GDI engine based on indicated mean effective pressure (IMEP). Energies 2017;10:368. http://dx.doi.org/10.3390/en10030368.

[49] Warey A, Gopalakrishnan V, Potter M et al. An analytical assessment of the CO_2 emissions benefit of two-stroke diesel engines. SAE Technical Paper 2016-01-0659; 2016. http://dx.doi.org/10.4271/2016-01-0659.

[50] Warey A, Gopalakrishnan V, Potter M et al. Comparison of different scavenging concepts on two-stroke high-speed diesel engines. In: Proceedings of THIESEL2016, conference on thermo-and fluid dynamic processes in direct injection engines. Valencia (Spain), 9–13th September 2016.